

Development of miniaturized pH sensor based on the pH-sensitive hydrogel HEMA-co-AA

by

Tran Thi Hong Hanh



Thesis submitted for the degree of
Master of Science

Department of Micro and Nano Systems Technology, IMST
Buskerud and Vestfold University College (HBV), Norway

December 2015

Abstract

The hydrogel biosensor is one of promising BIOMEMS (Biomedical Microelectromechanical system) devices with vast of applications in biomedical field. This project aims to develop a pH biosensor based on pH responsive hydrogels a piezoresistive pressure sensor capable of monitoring ambient pH as a signature of the physiological health status of a cell culture (*in vitro*), tissue or organ (*in vivo*). The hydrogel 2-hydroxyethyl methacrylate-*o*-acrylic acid (HEMA-co-AA) was chosen to be incorporated into a cavity of a piezoresistive pressure sensor. The hydrogel was synthesized and investigated separately within the fabricated SU8 photoresist cavity where hydrogel can only expand or shrink in one direction. When immersing the hydrogel into the pH buffers, the percentage of volume change of the hydrogel was determined indirectly by a profilometer. The hydrogel samples with thickness from 77-110 μm performed the expansion degree of 55-77% at low pH 2-4 and of 130-195% at higher pH 5-11. Both the equilibrium time and the maximum expansion of hydrogel samples were influenced by their thickness. Practical experiments also showed that there is a hysteresis of the hydrogel response which can be accounted for a delay of the protonation to deprotonation mechanism. Results indicated that the hydrogel sample after hydration should be stored in suitable pH buffer. The design of the front-end hydrogel sensor electronics and packaging procedure was made. The hydrogel HEMA-co-AA 4:1 (molar ratio) after characterization was in situ synthesized in the cavity of a piezoresistive pressure sensor. The hydrogel sensor was involved in two different packaging processes. Results showed an increase in the electrical signal of the hydrogel, proving that the hydrogel can generate a pressure on silicon diaphragm of the pressure sensor. The specific hydrogel incorporated into the cavity of the pressure sensor was reached to equilibrium status in approximately 7 hours. However, the hydrogel sensor could not stay stable in the solution for long period of time due to the properties of packaged adhesives toward solution. The problems were pointed out for future improvements.

Acknowledgments

First and foremost, I would like to express my deepest gratitude to my supervisor, Professor Erik Andrew Johannessen for his valuable advices, support and enthusiastic guidance. I would like to thank Professor Bjorn Torger Stokke for his supportive discussions during my thesis.

I would like to send my warm thanks to Lab Engineers working in Department of Micro and Nano Systems Technology. Specially, I would like to thank Zekija, Anh Tuan, and Ragnar not only for their helps in lab work but also for their encouragements.

I wish to acknowledge my BioMEMS group, Professor Urik , Agne, and Kristin for every support they have done for me during my time working as a member of this group. I will miss Friday-group-meeting.

Especially, I treasure any moment I spent with my friends in HBV and in Borre Campus. Their loves and wishes are something I will bring with in the journey of my life.

Finally, for my family, there is a non-stop love for them. Thank you for being a fulcrum for my whole life.

Contents

1	Introduction	11
1.1	Motivation	11
1.2	Research goal	14
1.3	Thesis outline	14
2	An overview of hydrogel	17
2.1	Introduction	17
2.2	The swelling-shrinking phenomena of pH -sensitive hydrogel	19
2.3	Theory for hydrogel modeling and simulation	22
2.4	Material considerations	26
2.5	Conclusion	28
3	Miniaturized-hydrogel characterization	29
3.1	Introduction	29
3.2	Materials	31
3.3	Methods	31
3.3.1	Hydrogel synthesis	31
3.3.2	Hydrogel characterization	36
3.3.2.1	Morphological properties of hydrogel in cavity	39
3.3.2.2	The swelling rate of HEMA-co-AA	39
3.3.2.3	Behavior of HEMA-co-AA	39
3.3.2.4	Hydration of different ratio of HEMA-co-AA	40
3.3.2.5	Hysteresis in the behavior of HEMA-co-AA	40

3.4	Results and discussions	40
3.4.1	Hydrogel synthesis	40
3.4.2	Hydrogel characterization	41
3.4.2.1	Morphological properties of hydrogel in cavity	41
3.4.2.2	The swelling rate of HEMA-co-AA	42
3.4.2.3	Behavior of HEMA-co-AA	43
3.4.2.4	Behavior of different ratio of HEMA-co-AA	46
3.4.2.5	Hysteresis in the behavior of HEMA-co-AA	48
3.5	Conclusions	50
4	Hydrogel based biosensor	53
4.1	Introduction	53
4.1.1	Hydrogel based sensor	53
4.1.2	Working principle of pH-hydrogel based sensor	57
4.2	Experimental work	59
4.2.1	Design of the hydrogel sensor and packaging	59
4.2.2	Materials & Components	61
4.2.3	Method	64
4.2.3.1	Experimental setup	64
4.2.3.2	Sensor assembly procedure	68
4.3	Result and Discussion	70
4.4	Conclusion	76
5	Conclusion and Future work	79
5.1	Conclusion	79
5.2	Limitation	82
5.3	Future work	82
	Bibliography	84

Abbreviation

AA	Acrylic acid
ATP	Adenosine triphosphate
DAQ	Data Acquisition card
DI	Deionized
DMAEMA	2-(Dimethylamino)ethyl methacrylate
HEMA	2-hydroxyethyl methacrylate
MEMS	microelectromechanical system
Op-amp	Operational amplifier
PBS	Phosphate Buffer Saline
PCB	Printed Circuit Board
pK_a	Acid dissociation constant
SU8	Name of a negative photoresist
UV	Ultra Violet

Chapter 1

Introduction

1.1 Motivation

pH inside the human body

The human blood and tissue fluid are buffered around a neutral pH of 7.4 at 37°C [1] to ensure the optimal conditions for functions of cells and tissues. This body has some control mechanism to self-regulate and maintain the pH value within a narrow range 7.35-7.45 (homeostatic systems). Since the entire metabolic process depends on a balanced pH , the pH of tissues and body fluids presents the state of human health, deviations above or below this pH range can signal potentially serious and dangerous symptoms or states of disease. For example, a depletion of oxygen due to circulation failure or the loss of blood flow (perfusion) may trigger anaerobic catabolism that temporarily attempts to restore energy production by producing lactic acid as an end product. An accumulation of lactate will reduce the pH below the threshold level. A lower pH condition may cause living cells to malfunction and even die. There is a relation between pCO_2 level in tissue, 1 mmHg change in pCO_2 results in 0.008 unit change in pH in the opposite direction [2]. The normal pCO_2 level in tissue is about 46 mmHg but can increase to 150 mmHg under severe hypoxia [3]. So approximately, it can be said that the pH of living tissue fluid can reach to a minima of pH 6.6.

Energy and Work

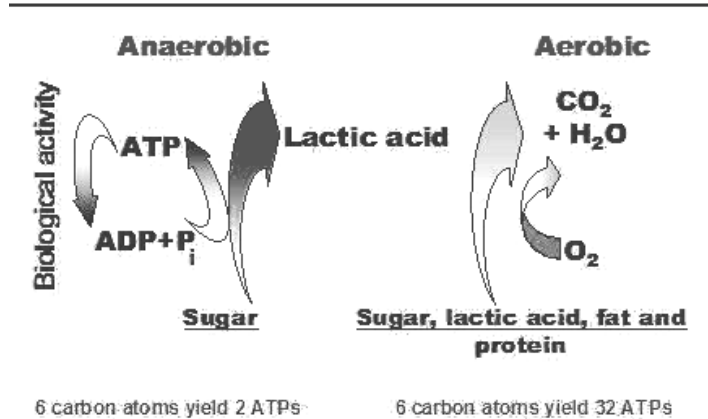
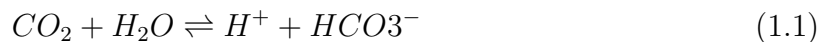


Figure 1-1: Anaerobic and aerobic (photo courtesy from Medbio.info)

Gastrointestinal ischemia

Gastrointestinal ischemia is a symptom happening when blood flow is inadequate to bring O_2 to the stomach and intestines [4,5]. After eating, the oxygen demand increases. Normally, a cell operating under aerobic catabolism consumes carbohydrates (sugar) and releases energy for the body in the form of adenosine triphosphate (ATP), and the by products H_2O and CO_2 which is removed by the blood flow (figure 1-1). However, when hypoperfusion occurs, the accumulation of CO_2 will induce the reaction (1.1) in the direction of forming more H^+ . An increase in H^+ concentration is a signal for a cell to activate the anaerobic catabolism. The anaerobic catabolism converts only sugar to lactic acid as the end product and less ATP than of aerobic catabolism. The agglomeration of lactic acid in turn makes the equation (1.1) to go reverse direction to create more CO_2 [6]. As a result both pCO_2 and pH decrease.



Gastrointestinal ischemia is either occlusive ischemia or non-occlusive ischemia. Occlusive ischemia results from the disrupted of blood flow (by abnormal twisting of the intestine or presence of thrombus figure 1-2) Non-occlusive ischemia results from systematic conditions such as circulatory shock, sepsis (toxic conditions by in-

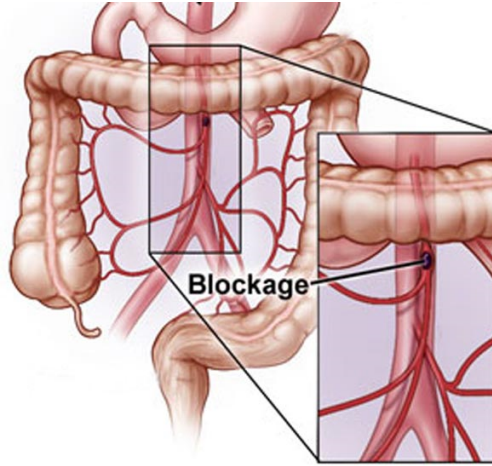


Figure 1-2: Gastrointestinal ischemia caused by thrombus (photo courtesy from pixshark.com)

fection) [6]. Diagnostic methods for ischemia are commonly based on evaluating the carbon dioxide concentration or $p\text{CO}_2$ by splanchnic angiography, duplex sonography, endoluminal pulse oximetry, tonometry [6], etc. These methods depend on complicated external apparatuses and measurement systems, not allow a real-time observation, and may cause pains for patients. Therefore, an implanted sensor for real-time diagnosis is the target for many current researches. A pH biosensor is among the solutions.

A pH biosensor

Developing a miniaturized pH sensor capable of measuring the acidity in cell cultures (in vitro) and in living tissue (in vivo) with the long term aim of targeting implantation in human subjects for real-time observing pH change inside human body should consider the biocompatibility of materials. Hydrogels can be a choice for sensing elements.

Hydrogels known as the biocompatible materials have been applied in the field of tissue engineering, regenerative medicine and drug delivery [7]. Hydrogels have been used for biomedical applications for their special properties such as having the similar structure to living cells as well as the sensitivity with specific stimuli in the target environment. Since the swelling rate of the hydrogel has a relation the its size [8], miniature MEMS (microelectromechanical system) devices in small scale

offer a unique opportunity for hydrogels to perform their sensing functions. Though implantable MEMS biosensors are few examples so far due to biocompatible challenges, micro-fabricated pressure sensors also have the potential for *in vivo* application [9]. The development of a *pH* biosensor based on *pH* responsive hydrogel and piezoresistive pressure sensor is highly motivated.

1.2 Research goal

The project aim is to develop a *pH* sensor based on a *pH*-sensitive hydrogel material for biomedical applications, particularly for measuring the acidity in cell cultures (*in vitro*) and in living tissue (*in vivo*) with the long term aim of targeting implantation in human body. It is expected to focus on (i) choosing the *pH*-sensitive hydrogel for optimized response in the desired *pH* range (ii) synthesis and characterization the hydrogel (iii) modification of an existing pressure sensor for the hydrogel incorporation, (iv) design of the front-end sensor electronics, (v) packaging the hydrogel sensor, (vi) test and measurement *in vitro* using standard buffer and *pH* solutions.

Feasibility of the project is supported by firm theory and previous reported work. The hydrogel that swells in response to the change of *pH* [10–13] is one member in the family of stimuli-sensitive hydrogel and has been demonstrated the ability to be incorporated into MEMS and other implantable devices for both *in vivo* and *in vitro* biomedical applications [9]. A piezoresistive pressure sensor with a membrane deformed by pressure when incorporated with hydrogels will transduce the response of *pH*-sensitive hydrogel to the change in solution to an electrical signal [14–18]. Incorporation between a hydrogel and a pressure sensor is possible and promising for either *in vivo* or *in vitro* applications.

1.3 Thesis outline

The thesis is mainly focus on development a *pH* biosensor based on the *pH*-sensitive hydrogel material. It is structured as follows. The first chapter is a general intro-

duction for the motivation for developing a miniature pH biosensor and goals of this thesis.

Chapter 2 introduces an overview of hydrogels. The chapter explains the special behaviors of pH -sensitive hydrogel, discusses the promising applications of hydrogels and hydrogel sensors in biomedical field. The chapter also introduces the basic theory for hydrogel simulation as well as some previous works on hydrogel modelling and simulation. The choice of the model hydrogel using in this project is also presented. In chapter 3, methodology utilized to synthesize and characterize the pH -sensitive hydrogel (2-hydroxyethyl methacrylate co acrylic acid) is described. This chapter also presents some elementary methods using to determine the swelling-shrinking degree of the pH -sensitive hydrogel and the necessity to understand the microscale hydrogel behavior are also discussed. Subsequently, the results for behaviors of this hydrogel are provided with detailed discussions. Chapter 4 presents working principle of hydrogel sensors as well as an explanation for capability of generating pressure of the hydrogel inside the confined cavity of the pressure sensor. The experiment work with the design, packaging and measurement methods used to characterize hydrogel sensor is addressed. Results and discussions are also given. Chapter 5 is the conclusion for the thesis. The chapter also discusses some future work possibilities for further improvements of hydrogel sensor.

Chapter 2

An overview of hydrogel

This chapter aims to give an overview of hydrogels, with emphasis on the promising applications of hydrogel in biomedical field as well as special behaviors of pH -sensitive hydrogels. The chapter also presents both elementary theory and antecedent studies on hydrogel modelling and simulation. Different types of hydrogels have been compared and a deliberate choice was made for the specific hydrogel used in this project: 2-hydroxyethyl methacrylate-co-acrylic acid (HEMA co AA). This hydrogel has the potential to work in a similar pH range of living tissue, it is biocompatible, and is neither really dangerous to handle in the preparatory steps.

2.1 Introduction

A hydrogel is defined as a three-dimensional cross-linked polymeric network that can contain a large amount of water within its structure. The polymer network comprises long chains called backbone which can be made up of one or more monomers, and which contains functional groups (side groups) which contribute to the unique behavior of hydrogel toward some sort of external stimuli. Long chains of backbone are linked to each other by cross-linking or by association bonds such as hydrogen bonds, and strong Vander Waals interaction [19] that creates a stable matrix. This matrix permits a hydrogel to hold up to 90% of water without dissolution.

Hydrogels have over the recent decades received a considerable amount of at-

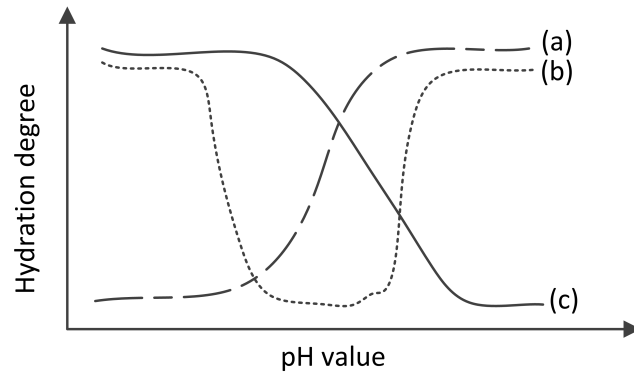


Figure 2-1: Behavior of hydrogel: acidic hydrogel (a), amphiphilic hydrogel (b) and basic hydrogel (c)

tention thanks to their ability to react with different environmental factors such as temperature, light, electrical field, ion concentration, pH , etc. They can be integrated into a physical transducer that is then transformed to a hydrogel sensor with potentially many applications, especially in chemical and biomedical fields, depending on the properties of the hydrogel. These sensors translate the physical swelling of a hydrogel to an electrical signal that can be read out by an associated electric circuit. It is expected that hydrogel sensors will have a promising position in biomedical applications. Many polymers are bio-compatible, and the ability of holding a large amount of water inside its structure makes it similar to natural living soft tissue. Other important properties are the inertness towards normal bioactivity, which makes them resistant towards degradation. Hydrogels can be easily prepared in any shape or form by casting, spin-coating, photo-patterning as well as integration into a transducer. The low cost of hydrogels may allow production of low cost disposable devices, and responds to the demand of real-time diagnosis in bio-medical and chemical applications.

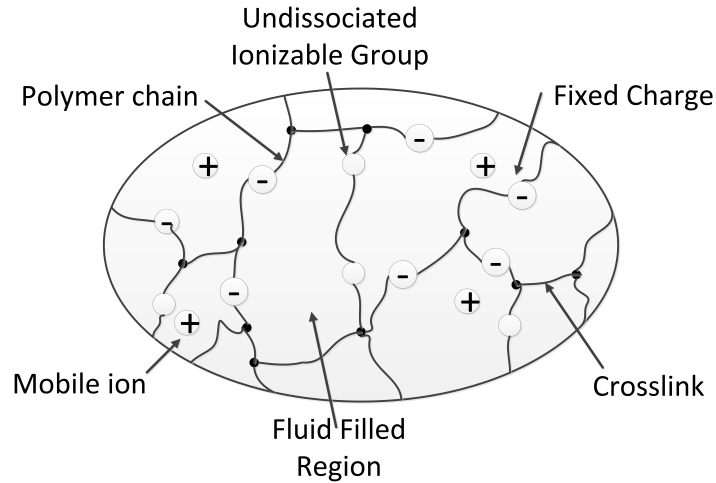
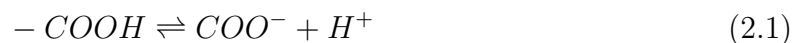


Figure 2-2: Hydrogel network with anionic side groups

2.2 The swelling-shrinking phenomena of pH -sensitive hydrogel

A pH -sensitive hydrogel is based on weak acid or weak basic side-groups that are attached to its backbone structure. These side-groups can be ionized as a function of pH , resulting in free counterions inside the hydrogel structure that can exchange with cations from the solution. The ion exchange follows the rule of maintaining charge neutrality inside the hydrogel. This means that when a hydrogel gives off ions to the surrounding solution, it will receive a similar amount of counterions in return. Therefore, inside the hydrogel, the concentration of counterions will increase, causing an osmotic pressure difference to develop between the gel and the solution. As a result, the hydrogel will swell until the elastic forces inside the hydrogel are in equilibrium with the osmotic pressure. Hydrogels with acidic side groups tend to expand with the increase of pH whereas hydrogels that contains basic groups, such as amphiphilic hydrogels, will expand at low pH and high pH value, and shrink in moderate pH (figure 2-1).



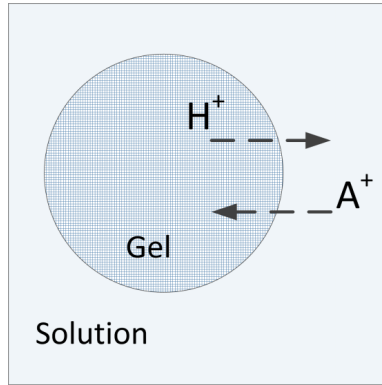


Figure 2-3: Ion exchange between gel and solution

A hydrogel network with acidic function groups is presented in figure 2-2. For a clearer explanation, we take an example with acidic hydrogel which has (-COOH) as the function group in its structure. When hydrogel is inside the solution, -COOH will be ionized following a reversible equation which is dynamic balance at equilibrium state, degree of ionization depends on the dissociation constant pK_a of the acid group. When pH in the solution increases, thus concentration of H^+ decreases, the balance of equation (2.1) will shift toward the right side, more H^+ to be produced inside the gel. H^+ from inner gel goes outside and in reverse, cation species from solution, for example A^+ goes inside to maintain the general electrical neutrality of the gel. The concentration of A^+ hence increase inside the gel and higher than that in the solution, the difference in concentration of A^+ causes osmotic pressure to make the gel expand. Oppositely, when pH in surrounding solution decreases, meaning H^+ concentration increases in the solution, the balance of equation (2.1) shift to the left side, therefore less H^+ to be generated. As a result, less A^+ will go inside to exchange with H^+ going outside, less osmotic pressure was generate so the gel tend to shrink. Ion exchange between hydrogel and solution is illustrated by figure 2-3.

The ionic strength has a large influence on the degree of hydrogel swelling. When a hydrogel with acidic side group, for example, hydroxyethylmethacrylate-co-acrylic acid (HEMA-co-AA), is exposed to pure water or low ionic strength solution, no osmotic swelling increase in the gel, although the pH of solution is higher than the pK_a of the acrylic acid (around 4.25). This can be explained by the electro-neutrality

maintaining mechanism in interior hydrogel, hydrogel tends to exchange proton to solution and take other counterions in reverse, but at low ionic strength, only protons exists in outside solution due to protolysis of water. Consequently, pH inside hydrogel network is low, most acid groups in protonated state (or uncharged state). There is no difference in concentration of counterions to cause osmotic pressure. When the ionic strength increases, hydrogels can exchange ions with solution, resulting in an increase of counterions concentration inside the hydrogel. The resulting increase in osmotic pressure causes the hydrogel to swell. When the ionic strength increase to high levels (1M-10M), the hydrogel will shrink due to the loss of the osmotic pressure between the gel and the solution, the solution now has osmotic pressures in the range of the osmotic pressure inside the gel.

Peppas et al [19] have derived a mathematical model to explain the swelling-shrinking of hydrogel based on Flory-Huggins thermodynamic theory, the rubber elasticity theory, and ionic interaction deviations. There are three contributions to the free energy of the system G : polymer-solvent mixing, elastic-retractive as the result of expansion of hydrogel and ionic free energies due to difference in concentration inside and outside hydrogel, expressed respectively by ΔG_{mix} , ΔG_{el} and ΔG_{ion}

$$\Delta G = \Delta G_{\text{mix}} + \Delta G_{\text{el}} + \Delta G_{\text{ion}} \quad (2.2)$$

Equation (2.2) can be rewritten in term of pressures,

$$\Delta \Pi = \Delta \Pi_{\text{mix}} + \Delta \Pi_{\text{el}} + \Delta \Pi_{\text{ion}} \quad (2.3)$$

In equilibrium state, the total energy reaches a minimum or zero

$$\Delta \Pi = \Delta \Pi_{\text{mix}} + \Delta \Pi_{\text{el}} + \Delta \Pi_{\text{ion}} = 0 \quad (2.4)$$

$$\Delta \Pi_{\text{mix}} + \Delta \Pi_{\text{ion}} = -\Delta \Pi_{\text{el}} \quad (2.5)$$

From equation (2.5) it is easy to see that the expansion-shrinkage of hydrogel due to the general tendency of hydrogel network to dissolve itself in solvent (mixing) and the

osmotic pressure caused by differences in ionic concentration inside and outside the hydrogel ($\Delta\Pi_{\text{ion}}$). But the osmotic pressure is much greater than the mixing force [10] (assume hydration due to mixing of hydrogel has been completed before pH starts to change) then it is possible to say that equilibrium of hydrogel is when elastic force of the network balance the osmotic force.

2.3 Theory for hydrogel modeling and simulation

The behavior of hydrogels have been modeled and simulated for several decades recently. pH -sensitive hydrogel simulation are basically based on the coupling of multi-field equations.

The problem of hydrogel simulation is to predict how much hydrogel expand-shrink in a certain condition. It is basically based on the coupling of multi-field equations. We can start with the mechanical field equation, in which the deformation of hydrogel can be determined (Chandrasekharaiah and Debnath, 1994) [20]

$$\rho \frac{\partial^2 u}{\partial t^2} + f \frac{\partial u}{\partial t} = \nabla \cdot \sigma + \rho b \quad (2.6)$$

where ρ is the effective density of the gel, u the vector of the displacements, f the viscous damping parameter between the solvent and the polymer-network, σ the stress tensor and b is the vector of body forces. Equation (2.6) has been derived containing term of osmotic pressure P_{osmotic} in the derived equation [21, 22]. P_{osmotic} is calculated in "Physical chemistry" book of Berry et al (1980) [23].

$$P_{\text{osmotic}} = RT \sum_k (c_k - c_k^0) \quad (2.7)$$

where c_k^0 is the concentration of the k^{th} ion in the stress-free state in the outside solution, c_k the concentration of k^{th} ion inside hydrogel. The ions considered in the computation of the osmotic pressure are ions with dominant concentrations. Concentration of H^+ and buffer ions are too small and can be ignored to make computation simple [21].

Concentration of ions inside the hydrogel is determined by a system of two equations. The first equation is Nernst-Planck equation. It is a conservation of mass equation used to describe the motion of the charged chemical species in a fluid medium. The flux of ions is described including diffusive flux (concentration gradients), electrical migration flux (gradient in electric potential), and convection flux (convection of the solven and the ions) [24, 25]

$$\Gamma_k = \phi \left[-\bar{D}_k \frac{\partial c_k}{\partial x} - \mu_k z_k c_k \frac{\partial \Psi}{\partial x} \right] + c_k U \quad (2.8)$$

where Γ_k is the flux of the k^{th} ion, ϕ the gel porosity, \bar{D}_k the effective diffusivity of the k^{th} ion inside the hydrogel, μ_k the ionic mobility and z_k the valence of the k^{th} ion, Ψ the electric potential, U the area-averaged fluid velocity relative to the polymer network and x is the coordinate system associated with the deformed hydrogel.

The second equation used to compute the concention of ions is either Donnan theory together with electro-neutrality condition or Poisson's equation. The Donnan theory (or Gibbs-Donnan equilibrium) describes the equilibrium that exists between two solutiona that are separated by a membrane. The expression for the Donnan equilibrium is given by equation (2.9) [24], and electro-neutrality equation given by equation (2.10). Solving equation (2.8), (2.9) and (2.10) can obtain all the concentration ions and fixed charge concentration. Poisson's equation is used in electrostatics to describe the potential energy field caused by given charges or mass density distribution (equation (2.11)). Solving equation (2.8) and (2.11)) can achieve ion concentrations and fixed charge concentration inside hydrogel.

The Donnan equilibrium equation is given by

$$\left(\frac{c_{k+}}{c_{k+}^0} \right)^{\frac{1}{|z_{k+}|}} = \left(\frac{c_{k-}^0}{c_{k-}} \right)^{\frac{1}{|z_{k-}|}} = \lambda \quad (2.9)$$

where c_{k+} and c_{k+}^0 are the concentrations of a positive ion inside and outside the hydrogel, respectively. Where c_{k-} and c_{k-}^0 are the concentrations of a negative ion inside and outside the hydrogel, respectively. z_{k+} and z_{k-} are the valences of the positive and negative ions, respectively. λ is termed as the Donnan partitioning

ratio.

The electro-neutrality equation is given by

$$\sum_{k=1}^n c_k z_k + c_f z_f = 0 \quad (2.10)$$

where c_f and z_f are the concentration and valence of fixed charge group inside the hydrogel structure.

The Poisson's equation is given by

$$\frac{\partial^2 \Psi}{\partial x^2} = -\frac{F}{\epsilon \epsilon_0} \left(\sum_{k=1}^n c_k z_k + c_f z_f \right) \quad (2.11)$$

Where F is Faraday's constant, ϵ , ϵ_0 are relative dielectric constant and vacuum dielectric constant of solvent.

The system of these equations described above is called the system of chemo-electro-mechanical equations, used to describe the swelling and shrinkage of hydrogel. It have been studied and solved by Wallmersperger et al (2001-2015) by numerical simulation [10, 19, 26, 27]. In this model, the author used the Nernst-Planck equation to describe the chemical field, and the Poisson's equation for the electrical field and mechanical field equations. Hua Li et al (2004) solved a similar model with Meshless Methodology Development called Hermite-Cloud Method (numerical technique) [22]. Kang et al (2008) uses Comsol-Multiphysics (simulation software) combined with Matlab software to solve model of chemo-electro-mechanical multi-field including Nernst-Planck equation, Donnan theory and elastic mechanics without considering Poisson's equations [28]. Sudipto et al (2002) reported an equilibrium and a kinetic model based on Donnan theory [10], but soon replaced the Donnan theory by a kinetics model based on chemo-electro-mechanics in 2004. The improved model used Poisson's equation instead Donnan theory, explaining that the Donnan theory is typically valid only at the boundaries of the gel may not be correct to determine the ionic concentrations inside hydrogel structure, especially for smaller gels where the concentration gradient within the gel is more steeper compared to that in larger gels and so is the electric potential. This model is similar to the model of Wallmersperger

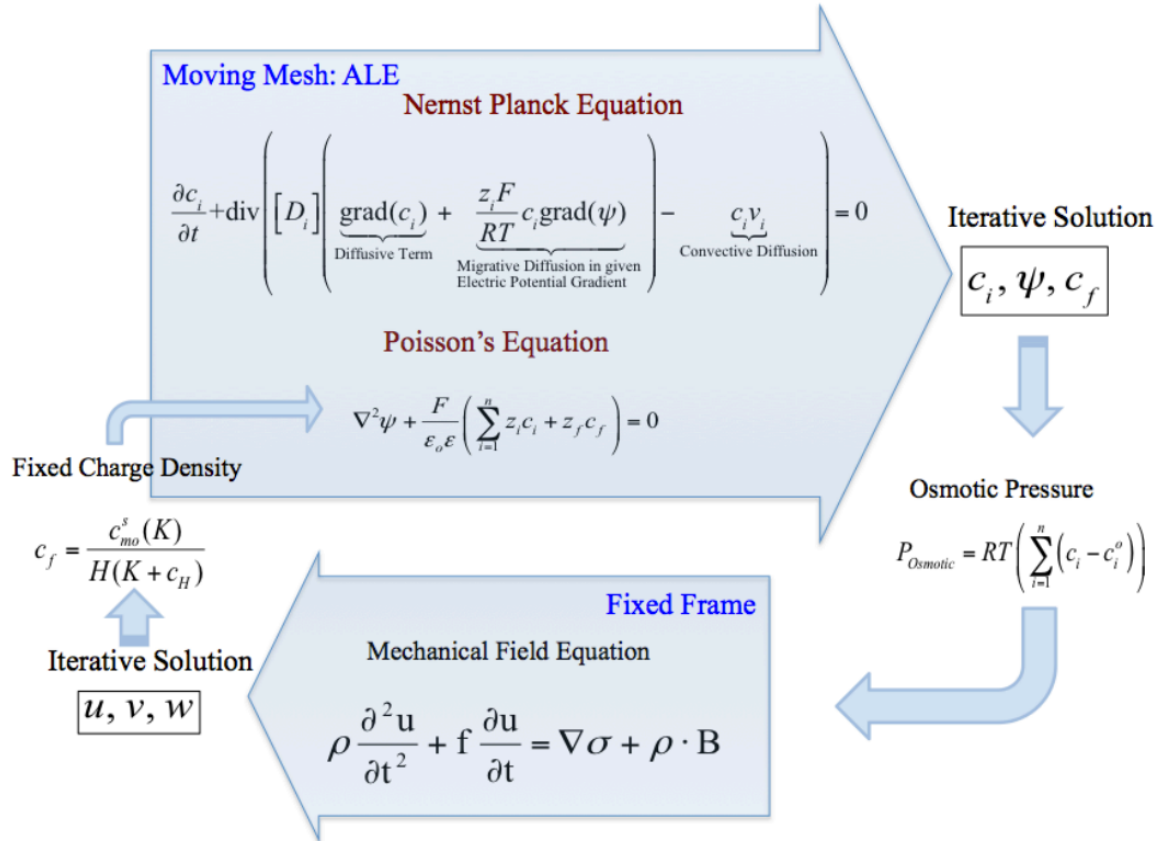


Figure 2-4: Coupling between different modules within Comsol in moving mesh and fixed frames required for hydrogel simulations [30]

mentioned above [21]. Suthar in his thesis (2009) used Comsol Multiphysics, employing a moving mesh method for 3D geometry, the FEM simulation was performed to account for large swelling of the pH sensitive hydrogel. Studies of Suthar have also been reported in [29, 30] (2013).

A flow diagram explaining his work on hydrogel simulations in Comsol multiphysics is illustrated in figure 2-4, showing a whole relationship between the chemo-electro-mechanical system of equations. The coupling of the Nernst Planck equation and the Poisson's equation can generate the solution for the ion species concentrations c_i , the fixed charge concentration c_f and the electrical potential which in turn permit us to compute the osmotic pressure $P_{osmotic}$, the main force that cause expansion/shrinkage within the hydrogel. $P_{osmotic}$ is used in mechanical field equations to solve for the deformation of a hydrogel which again induces the change of fixed charge concentration and hence the solution of Poisson's equation. In addition, Thong Trinh

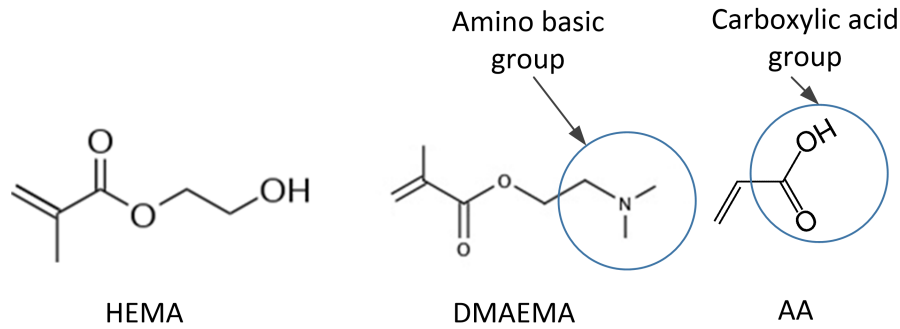


Figure 2-5: Chemical structure of HEMA, DMAEMA, AA

et al (2006) attempted to investigate the behavior of silicon piezoresistive pH sensor which relies on the pH sensitive property of a hydrogel. They simulated the silicon membrane deflection and the stress inside the membrane using finite element method (ANSYS software) [21, 28].

2.4 Material considerations

The suitably chosen hydrogel should refer the purpose of this project to develop a biosensor. Therefore, it is important to consider both the biocompatibility of materials as well as the appropriate working range of hydrogel can respond to. pH range for living tissue in normal condition is around 7.4 and can be reduced to 6.6 as mentioned in chapter 1, section 1.1.

The most widely used biomedical hydrogel is water swollen, crosslinked poly(2-hydroxyethyl methacrylate) (pHEMA). It shows resistance to degradation and is permeable to most metabolites. In addition, it is not absorbed by the body, withstands heat sterilization without damage, and can be prepared in a variety of shapes and forms. Other important hydrogels are acrylamides, co-monomers of acrylic acid or methacrylic acid with other co-monomers [19].

HEMA-co-AA was a deliberate choice among 2-hydroxyethyl methacrylate co Acrylic acid (HEMA-co-AA), and 2-hydroxyethyl methacrylate co 2-(Dimethylamino)ethyl methacrylate (HEMA-co-DMAEMA). The difference between these HEMA based hydrogels is the functional group of the co-monomer. While AA contains carboxylic acid

Table 2.1: Comparison of HEMA-co-DMAEMA and HEMA-co-AA

Object	HEMA-co-DMAEMA	HEMA-co-AA
Functional group	Amino $-N-(CH_3)_2$	Acid $-COOH$
Ionic monomer	DMAEMA	AA
pK_a of DMAEMA	8	4.25
Behavior when increase	Shrink	Expand

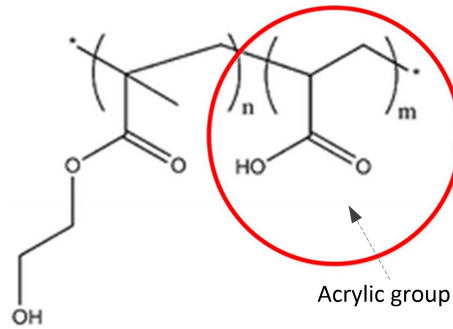


Figure 2-6: Chemical structure of HEMA-co-AA

groups which make the gel expand when pH increase, DMAEMA contain basic amino basic groups which induce the gel to expand when pH decrease. HEMA-co-DMAEMA with the pK_a of DMAEMA around 8, is reported to have acid dissociation constant pK_a around 7 [26] which means this gel will significantly change around this value. This value of pK_a is very close to normal pH of living tissue (pH 7.4), matching with the range of pH change 6.6 - 7.4 inside living tissue. HEMA-co-AA has the acid dissociation constant pK_a of AA is 4.25 [31], the pK_a of HEMA-co-AA was experimental determined by this project is approximately 5.5-6 which is expected to drastically swell-shrink in range of pH 4 - 8 (chapter 3). Therefore, HEMA-co-AA can also be usable in the working range of living tissue. On the other hand, DMAEMA is extremely toxic that adults can be killed if inhaling while AA is only classified as acute toxic (information given in specification by Sigma-Aldrich Company). For safety reasons, HEMA-co-AA was chosen. Although the pH range is not optimal, it will work as a proof-of-concept material within the aim of this project. The chemical structure of HEMA, DMAEMA, AA are illustrated in figure 2-5. A comparison of the two mentioned hydrogels is presented in table 2.1.

Finally, throughout this project, hydrogel HEMA-co-AA was used. It is synthesized from a monomer HEMA, co-monomer AA, the crosslinker tetraethylene glycol dimethacrylate (TEGDMA), and finally the photoinitiator 2,2-dimethoxy-2-phenylacetophenone (DMPAP). The synthesized hydrogel should have the structure as presented in figure 2-6.

2.5 Conclusion

Hydrogels in general and pH -sensitive hydrogels in particular are relative new materials with a potential for integration with physical sensors, transducers or actuators in the field of BioMEMS. The kinetics of swelling-shrinking of hydrogels can be explained and different model have been built to describe this behavior in detail. Modellings and simulations of hydrogels will permit researchers to predict the properties of hydrogel for sensors with high accuracy. In this project, the hydrogel HEMA-co-AA was chosen as the model component used for integration into a pH sensitive biosensor.

Chapter 3

Miniaturized-hydrogel characterization

This chapter introduces some methods to determine the swelling-shrinking degree of the *pH*-sensitive hydrogel and discusses the necessity to understand the miniature hydrogel behavior in constraint condition. As the main parts of the chapter, the methodology used to synthesize and characterize the *pH* sensitive hydrogel HEMA co AA that was chosen as the model component in this project are presented. Subsequently, the results for behaviors of this hydrogel are provided with detailed discussions.

3.1 Introduction

Hydrogels have been known to science for a long time and are currently being investigated for use in a wide range of applications. However not all is known about hydrogels, especially when it is scaled down to the micro range. Also, incorporating stimuli-sensitive hydrogel into physical microtransducers, will take the advantage of translating the mechanical properties of the gel to an electronic or optical read-out platform providing a source of data. Therefore, there is a need to understand the behavior of confined hydrogel. For example, the response time of a hydrogel, referred to (3.1) (Fick's second law of diffusion), depends on the diffusion distance x and the diffusion coefficient D of the respective ions and molecules involved in the swelling

process. Thus, with the purpose to reduce the response time, diffusion distance should be reduced. This can be achieved by downsizing the hydrogel that is integrated into the sensor. It would be interesting to know the behavior of micro-scale hydrogel in a constraint condition.

$$t = \frac{x^2}{D} \quad (3.1)$$

Many methods used to determine the hydration of *pH* sensitive hydrogel have been approached. Most of these rely on a free expansion of the hydrogel. A change in volume of can be measured traditionally by weighing the hydrogel, or optically by imaging sample movement using a microscope. The measurements were improved by more accurate methods when incorporating hydrogels into transducers which allow converting signal of swelling/shrinking from hydrogel to electrical signal. Two basic principles for evaluating changes of hydrogels by transducers were mentioned in [32], including transducers based on mechanical work performed by hydrogel swelling and shrinking and transducers based on observing changes in properties of free swelling gels. The mechanical work induced by the expansion and shrinkage of hydrogels can be incorporated with microcantilevers, bending plate transducers, etc. The changes in properties of free swelling gels such as optical properties, mass can be the main factors to determine the hydration degree of hydrogel themselves when they are integrated into relevant transducers. Some possible transducers are optical transducers, conductometric transducers [33], oscillating transducers such as quartz crystal micro balance [34], magnetoelastic sensor [35]. The changes in properties of hydrogels can be observed indirectly by modifying the hydrogel surface with a coating material or from embedded objects implanted (nanoparticle surface coating) or by fluorophores labelling. The changes of hydrogels induces the changes (position, intensity or optical properties) of these objects and are then measured by optical transducers.

In this project, the hydrogel is synthesized in microscale, constrained in all direction but one opening to the environment. Characterization for miniaturized-hydrogel was determined using profilometer with vertical resolution down to 1 Å. The same

method was used in the work of S. Payen (2007) [26].

3.2 Materials

The hydrogel hydroxyethyl methacrylate-co-acrylic acid (HEMA-co-AA) was synthesized from: 2-hydroxyethyl methacrylate, HEMA, (128635, Sigma-Aldrich, USA), acrylic acid, AA, (147230, Sigma-Aldrich, USA), tetraethylene glycol dimethacrylate, TEGDMA, (86680, Sigma-Aldrich, USA), and photoinitiator 2,2-dimethoxy-2-phenylacetophenone, DMPAP, (196118, Sigma-Aldrich, USA). *pH* buffers from 2-12 were prepared from ortho-phosphoric acid (100573, Merck, Germany), sodium phosphate monobasic monohydrate and sodium phosphate dibasic dehydrate (S9638 and 71643, Sigma-Aldrich, USA). Ionic strength of all *pH* buffers was adjusted by sodium chloride (746398, Sigma-Aldrich, USA). The photolithography process used chemicals offered in cleanroom of Buskerud and Vestfold University: SU8100 (Micro Resist Technology GmbH, Germany), developer mr-Dev 600 (R815100, Micro Resist Technology GmbH, Germany), and other chemicals.

3.3 Methods

3.3.1 Hydrogel synthesis

SU8 cavity fabrication

A negative photoresist SU8-100 was used to fabricate the microcavities used to synthesize the hydrogel. Negative photoresist refers to photoresist that will be crosslinked for the part cured under UV light, parts not exposed to UV light will remain soluble and can be washed away by developer. SU8 derives its name from consisting of 8 groups of epoxy in its structure (figure 3-1). By means of photolithography techniques, square cavities were formed with 1400 μm sides and depth of 100-150 μm . Two different processes have been set up: the first process to create SU8 wall on silicon wafer (SU8-silicon) (figure 3-2a, b), the second one to form SU8 wall

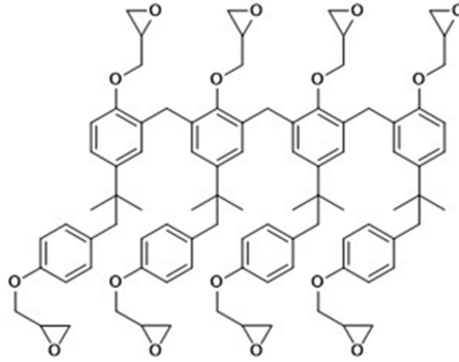


Figure 3-1: Structure of photoresist SU8

on a SU8 base (SU8-SU8) (figure 3-2c).

The first photolithography process is described as following. A silicon wafer was firstly pretreated by rinsing carefully with acetone, iso-propanol and deionized (DI) water before pre-baking at 200°C in 10 minutes to drive off any moisture on the wafer surface. About 10 ml of SU8-100 was spin coated using the SP100 Spin Coater with process parameters shown in figure 3-3. A soft-baking was followed at 75°C in 25 minutes and 105°C in 55 minutes to increase the viscosity of photoresist and ensure the uniform thickness distribution on silicon wafer. A photomask with different transparent and opaque regions was used in exposure step to allow UV light only on expected area of photoresist. This happens in 65 seconds under UV lamp with light intensity 8.5 mW/cm^2 . Wafer was then post-baked at 75°C in 12 minutes and 105°C in 12 minutes. After post-baking, it was very important to leave the wafer to cool down before developing to prevent any broken in structure (due to thermal shock in such a thick photoresist layer). Developing step was conducting in Developer mr-Dev 600 in 10 minutes. The wafer was rinsed with isopropanol, dried by nitrogen and checked to make sure a complete development by microscope. Hard-baking was an optional step for 5 minutes. The second process for SU8-SU8 cavities follows the same steps but adding one layer of SU8 spin coated on silicon wafer without developing before adding another SU8 layer.

Hydrogel synthesis

Pre-hydrogel solutions were prepared consisting of HEMA and AA at mole ratio

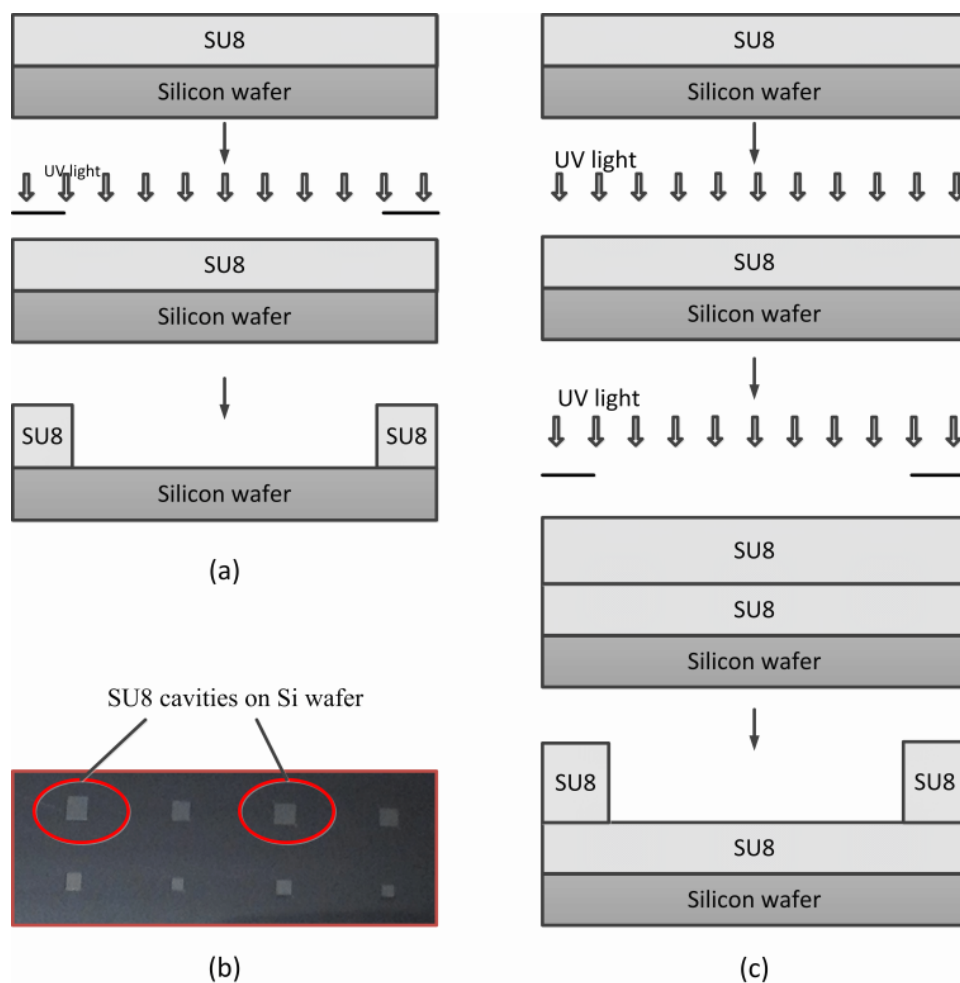


Figure 3-2: (a) SU8-silicon process, (b) SU8 cavities on silicon wafer, (c) SU8-SU8 process

6:1, 4:1, 2:1, 1.67% crosslinker TEGDMA and 3% photoinitiator DMPAP to the total weight. An amount of pre-hydrogel solution was injected manually into prepared cavities by using a micropipette and exposed to UV light intensity of 12 mW/cm^2 in 550 seconds to achieve a complete polymerization as illustrated in figure 3-4 [10,13,26]. Synthesized hydrogels were synthesized individually on wafer and diced for further testing (figure 3-5). All the hydrogel samples were stored in nitrogen cabinet before testing.

Phosphate-buffered saline (PBS) preparation

A pH buffer is the solution in which a molecule tends to either bind or release ions in order to maintain a particular pH . It contains a mixture of a weak acid and

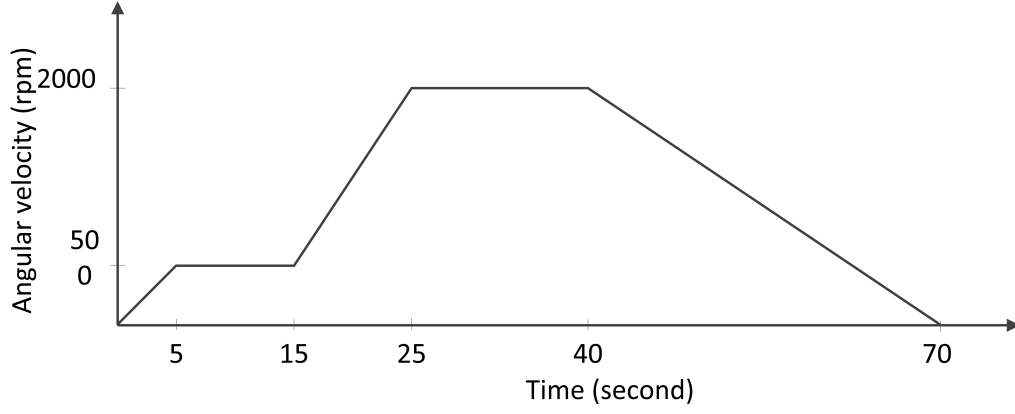


Figure 3-3: Spin coating program

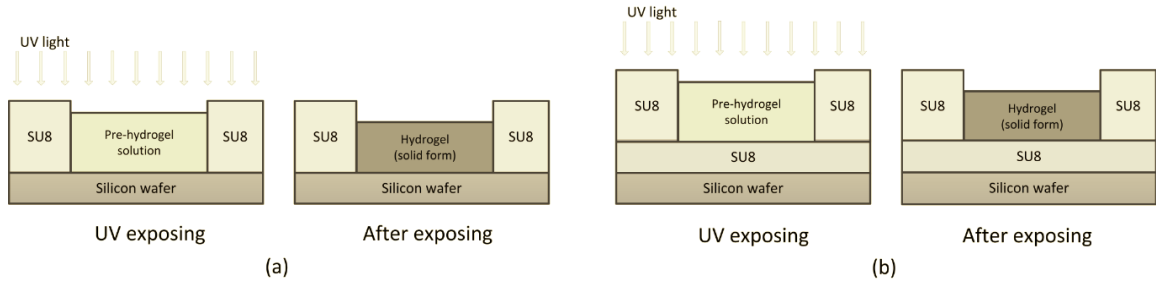


Figure 3-4: Hydrogel synthesized (a) in SU8-silicon cavity, (b) in SU8-SU8 cavity

its conjugate base, or vice versa. The test solution used in this study was based on a phosphate-buffered saline (PBS) which simulate the composition and pH of a human body fluid known as the interstitial fluid, which resides in living tissue. PBS buffers of different pH were prepared from ortho-phosphoric acid, sodium phosphate monobasic monohydrate and sodium phosphate dibasic dehydrate. Ionic strength was adjusted to 200 mM by using sodium chloride. pH buffers were prepared based on pairs of $H_3PO_4/H_2PO_4^-$, $H_2PO_4^-/HPO_4^{2-}$, HPO_4^{2-}/PO_4^{3-} and their dissociations shown in equations (3.2), (3.3), (3.4). In these chemical equations, K_a represents for acid dissociation coefficient, pK_a is the negative logarithm of K_a . The smaller pK_a , the more acidic the substance). In solution, along with the dissociations of phosphate salts, there always exists the dissociation of water, however, water dissociation coefficient is rather small compared to the others, so it is assumed to be ignored in equation (3.5).



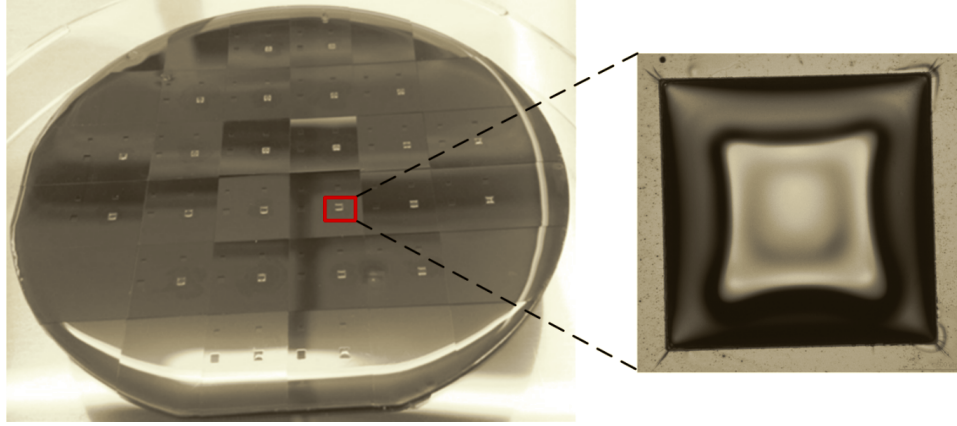
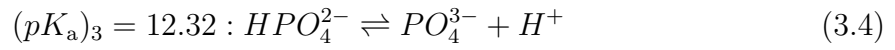
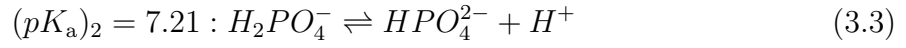


Figure 3-5: Synthesized hydrogel on diced wafer



The ratio of the amount of buffer components were calculated based on the chemical equations for each pair of acid/conjugated base.

For $H_3PO_4/H_2PO_4^-$:

$$pH = (pK_a)_1 + \lg \frac{[H_2PO_4^-]}{[H_3PO_4]} \quad (3.6)$$

$$\frac{[H_2PO_4^-]}{[H_3PO_4]} = 10^{(pH - (pK_a)_1)} \quad (3.7)$$

For $H_2PO_4^-/HPO_4^{2-}$:

$$pH = (pK_a)_2 + \lg \frac{[HPO_4^{2-}]}{[H_2PO_4^-]} \quad (3.8)$$

$$\frac{[HPO_4^{2-}]}{[H_2PO_4^-]} = 10^{(pH - (pK_a)_2)} \quad (3.9)$$

For HPO_4^{2-}/PO_4^{3-} :

$$pH = (pK_a)_3 + \lg \frac{[PO_4^{3-}]}{[HPO_4^{2-}]} \quad (3.10)$$

$$\frac{[PO_4^{3-}]}{[HPO_4^{2-}]} = 10^{(pH - (pK_a)_3)} \quad (3.11)$$

Since the value of the buffer pH is around at the logarithmic scale pK_a of acid, PBS buffers from phosphoric and its salts can vary from 2-12.

3.3.2 Hydrogel characterization

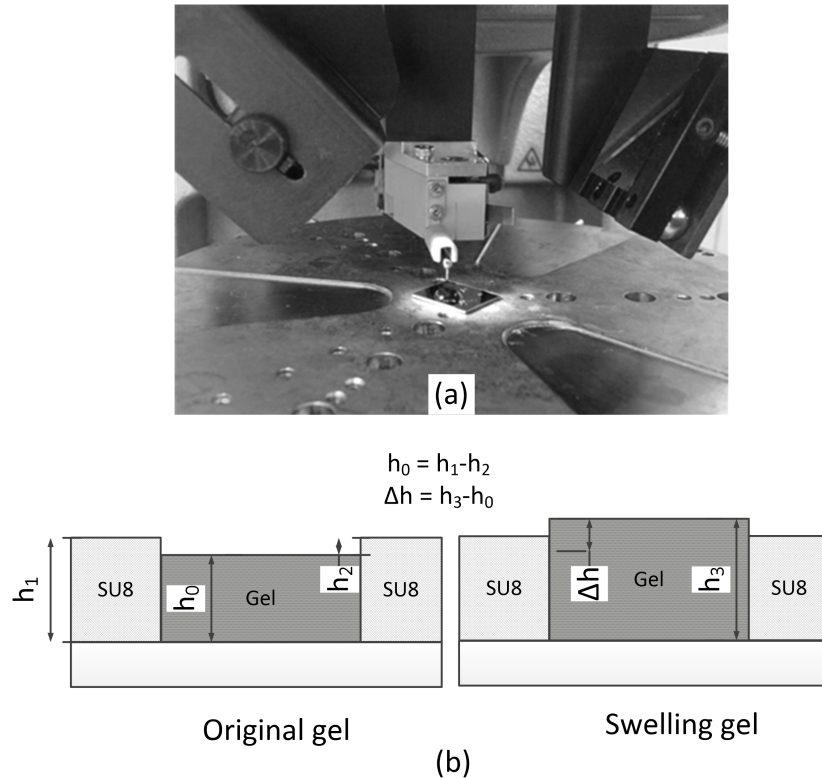
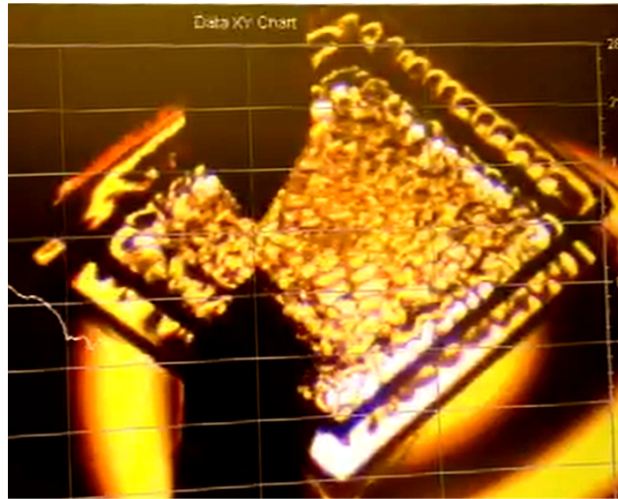


Figure 3-6: (a) Measuring hydrogel thickness by profilometer, (b) Hydrogel thickness calculation

The hydrogel samples were synthesized in a cavity where it was only allowed to swell-shrink in one direction. Thus, the changes in volume of the hydrogel sample were indicated by measuring the changes in thickness of the sample. The Dektak 150 Surface Profilometer (Veeco Instruments Inc, USA) is the equipment used to characterize the hydrogels in these experiments. The vertical range and theoretical resolution of the Dektak 150 are $524 \mu\text{m}$ and 1 \AA respectively. In this experiment, the profilometer was set to measure in $524 \mu\text{m}$ with a stylus force 1 mg . The thickness

of the hydrogel samples before and after exposure to a particular pH buffer were measured indirectly. A sketch of how to measure and calculate the hydrogel thickness is shown in figure 3-6 where h_0 is the initial thickness of hydrogel, h_1 the depth of cavity, h_2 the depth of cavity containing hydrogel dried hydrogel inside, h_3 the depth of cavity and swelling gel, Δh is the displacement of hydrogel. As a result of swelling inside confined cavity, surface of hydrogel samples were not flat, but rough. In order to measure accurately for specific positions across a polymer surface, measurements were made through two diagonals of square cavity (figure 3-7c) . The samples were immersed in pH buffer during the measurement to prevent dehydration when exposed to air. A clear image of hydrogel under the needle of the profilometer and typical results by presented on the monitor of profilometer system can be seen in figure 3-7a, b.



(a)

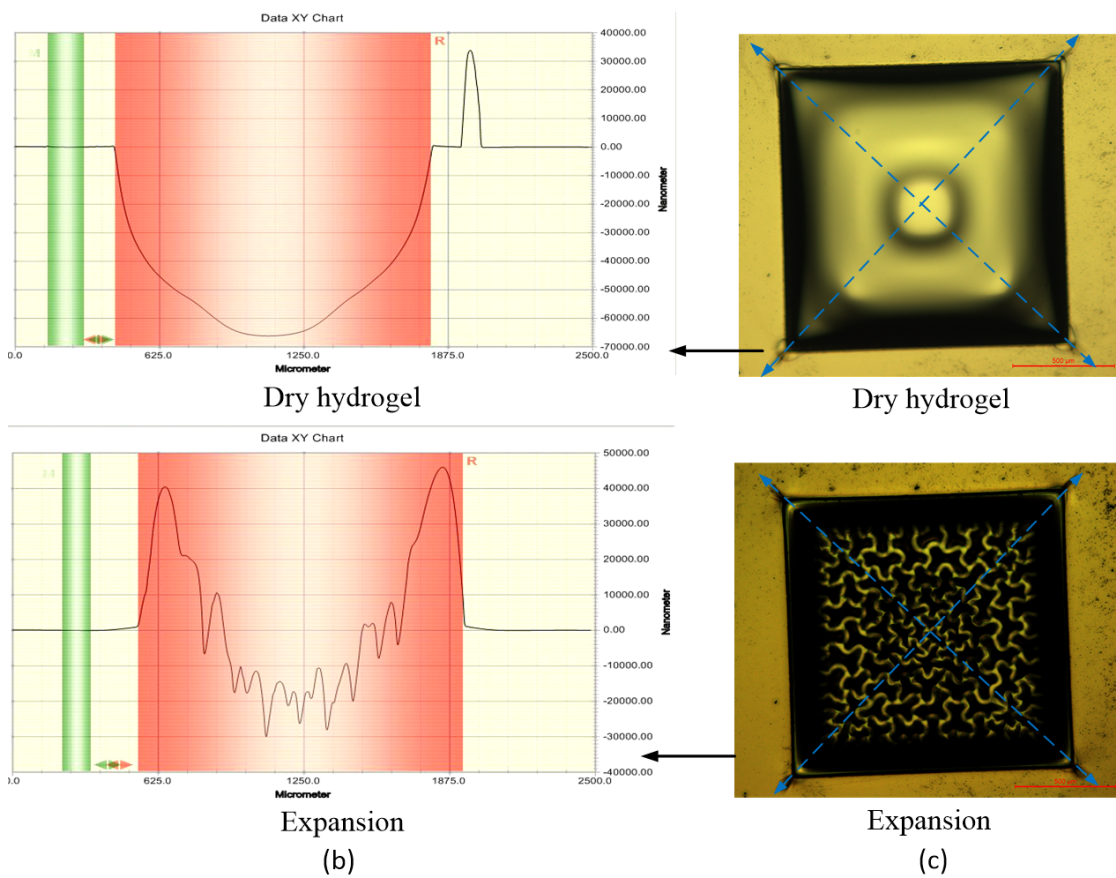


Figure 3-7: The measurement of thickness of hydrogel with a profilometer. (a) Results showing the "dry state" after synthesis, and (b) after immersion in pH buffer and subsequent expansion. (c) The hydrogel surface was measured through two diagonals

The hydrogels were characterized as a function of pH range, response/equilibrium time, hydration of different ratio of HEMA-co-AA, and for any hysteresis behavior.

3.3.2.1 Morphological properties of hydrogel in cavity

A sample of hydrogel synthesized in a cavity was used to observe change in thickness and shape of hydrogel inside the cavity due to hydration and dehydration process. Hydrogel was first in a dry state and then dropped solution on surface to observe any change. Photos were taken under microscope for each 20 seconds.

3.3.2.2 The swelling rate of HEMA-co-AA

Two samples of HEMA-co-AA at ratio 4:1 were immersed in pH buffer 3.91 and 6.92 with thickness 61 μm and 77 μm respectively and measured after each two minutes until 90 minutes and then almost 28 hours later to see how much time for the hydrogel samples to get in equilibrium status and how differently hydrogel samples behave in different pH buffers. Hydration degree is calculated by equation 3.12

$$H(\%) = \frac{\Delta V}{V_0} = \frac{h}{h_0} \quad (3.12)$$

Where $H(\%)$ hydration degree, ΔV change in volume, V_0 initial volume of hydrogel as dry state, h change in thickness, h_0 initial thickness of hydrogel, h is calculated as showed in figure 3-6.

3.3.2.3 Behavior of HEMA-co-AA

Experiment 1 was to determine a general behavior of hydrogel in a wide range pH and to figure out the pH range for drastic swelling of HEMA-co-AA. Different hydrogel samples were dipped inside pH buffers from 2-11 sequentially. Changes in volume of polymer samples in pH buffers were observed after 18, 38, and 44 hours. Then, hydrogel samples had been dried naturally in air and stored in nitrogen cabinet for 23 hours before being rehydrated in relevant pH solutions during 4.5 hours and measured the thickness changes.

Experiment 2 with two samples, moved from one pH buffer to other pH buffers in every 30 minutes. Experiment 3 was implemented as experiment 2 but in 60 minutes.

These two experiments were compared to each other and compared to experiment 1 to determine an actual pH range.

3.3.2.4 Hydration of different ratio of HEMA-co-AA

HEMA-co-AA hydrogel samples were prepared in different ratio 2:1, 4:1, 6:1. Samples were moved from pH 2.29 to 11.04 and stay 30 minutes in each buffer. Changes in thickness were recorded.

3.3.2.5 Hysteresis in the behavior of HEMA-co-AA

Samples stayed 30 minutes in each buffer for pH from pH 2.29 to 11.04,. Experiments were repeated but sample were left in 60 minutes in each buffer to make a comparison.

3.4 Results and discussions

3.4.1 Hydrogel synthesis

Both SU8-silicon and SU8-SU8 cavities were prepared, side of square cavities 1.4 mm , depth 100-150 μm . Hydrogel samples were successfully synthesized inside those cavities. pH buffers were prepared from 2-12, measured by pH electrode. Hydrogel samples were characterized in both SU8-silicon and SU8-SU8 cavities. Experiments showed that in SU8-silicon, characterization cannot be done properly due to a difference in adhesion of hydrogel samples to SU8 wall and silicon bottom, resulting in buckling when samples swelled in $pH > 7$. These below results were recorded with samples in SU8-SU8 cavities. The results achieved on the characterization of the hydrogel are with the SU8-SU8 cavity.

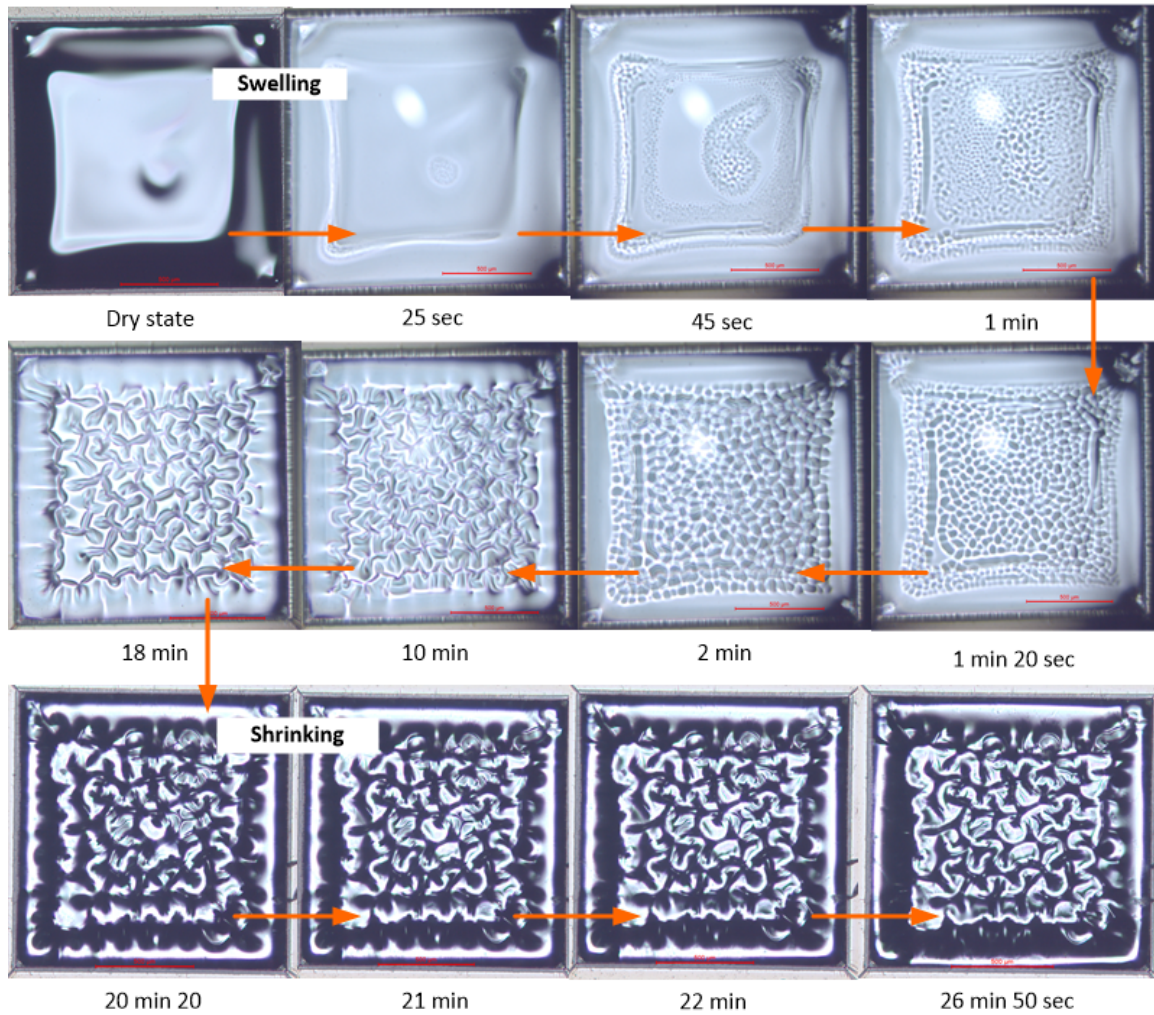


Figure 3-8: Hydration and dehydration of hydrogel under microscope

3.4.2 Hydrogel characterization

3.4.2.1 Morphological properties of hydrogel in cavity

Observing the swelling and shrinking of the hydrogel sample due to hydration and dehydration process in the cavity, many creases were formed on the surface of hydrogel (figure 3-8). The hydrogel in a confined volume (cavity) cannot spread its structure in all directions as in the conditions of free-expansion. They were forced to expand in one direction, so they tend to fold the structure forming creases on the surface. This may not happen in case of free expansion.

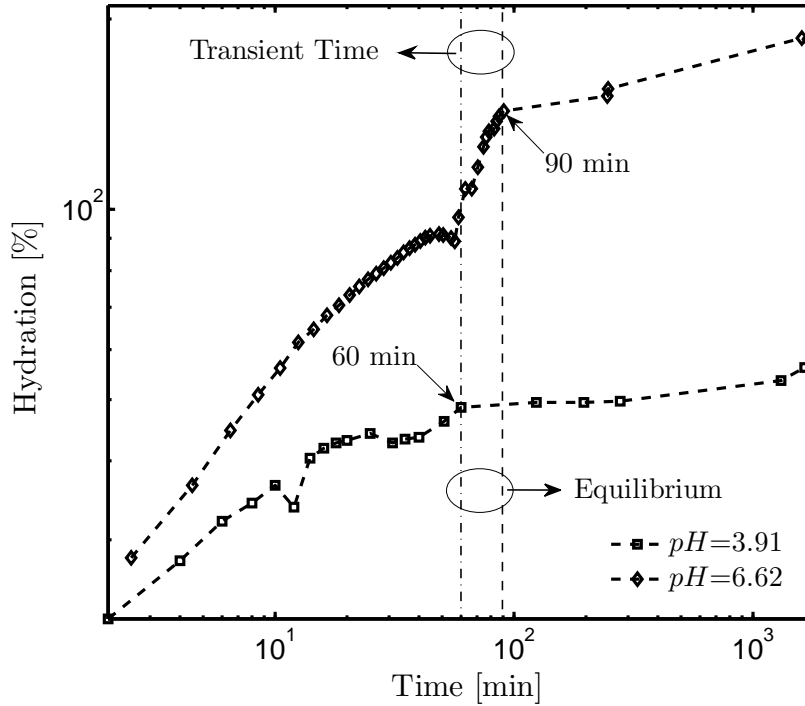


Figure 3-9: Swelling rate of hydrogel HEMA-co-AA

3.4.2.2 The swelling rate of HEMA-co-AA

Studying swelling rate of HEMA-co-AA (4:1) (figure 3-9) shows that gel from initial state (dry) swell dramatically fast in first 30-60 minutes. In $pH=3.91$, for the first 30 minutes, it swells to 43% of initial volume, and to 49% in 60 minutes. In $pH=6.62$, the sample swells to 82% in first 30 minutes and to 108% in 60 minutes (Table 3.1).

Results from figure 3-9 show that thinner hydrogel swells (hydration) faster than thicker one in specific time. The reason is thin layer of hydrogel has shorter diffusion paths for ions from outside to diffuse into the whole structure of the gel. It also can be seen that higher pH values make the gel swell stronger, resulting in higher hydration degree at equilibrium status than in lower pH . At low pH , little acidic groups are protonated, so the exchange of ions with surrounding solution happens very limited. The main driving force to induce hydrogel to expand and withdraw water into its structure is mixing force. The role of the osmotic pressure in this case is not significant. Oppositely, in high pH , more acid groups of the gel are protonated, more proton H^+ to be released to exchange with cations from solvent, as a result,

Table 3.1: Hydration of HEMA-co-AA (4:1) in pH 3.91 and pH 6.62

Parameters	pH 3.91	pH 6.62
Thickness (μm)	61	77
Hydration in 30 minutes (%)	43	82
Hydration in 60 minutes (%)	49	108
Hydration in 90 minutes (%)	49	143

osmotic pressure increases, causing the gel to expand much more than in low pH buffers. It took approximately 60 minutes, 90 minutes for the hydrogel sample of thickness 61 μm , 77 μm to get in equilibrium state, respectively.

The characteristic time constant of polyelectrolyte gels in presence of buffer ions was investigated by Lesho and Sheppard [36], given by

$$\tau_{\text{bdr}} = \frac{\delta^2}{\pi^2 D_{\text{HB}}} \left[1 + \frac{\beta_{\text{gel}}}{(1 + H_0)\beta_{\text{HB}}} \right] \quad (3.13)$$

δ is gel thickness, D_{HB} diffusivity of the buffer molecule into the gel, H_0 hydration, gel buffer capacity of the hydrogel, β_{HB} buffer capacity of the buffer solution. Assume that in these experiments, only thickness of the sample changes:

$$\frac{\tau_1}{\tau_2} = \left(\frac{\delta_1}{\delta_2} \right)^2 \quad (3.14)$$

To these experiments, there are two samples with thickness $\delta_1=61 \mu\text{m}$ and $\delta_2=77 \mu\text{m}$ having constant time $\tau_1 = 60$ minutes and $\tau_2 = 90$ minutes respectively. The ratio $\left(\frac{\delta_1}{\delta_2}\right)^2 = 0.63$ and $\left(\frac{\tau_1}{\tau_2}\right) = 0.67$ are nearly equal.

3.4.2.3 Behavior of HEMA-co-AA

Acrylic acid has a pK_a of around 4.25, and figure 3-10 shows that the reference behavior of acrylic acid gel in pH solutions, drastically swells in pH 4-7. Thus a prediction was made that the hydrogel HEMA-co-AA will significantly swell around the same range of pH . Sample list and swelling degree (or hydration degree) of HEMA-co-AA in pH buffers were presented in table 3.2 and figure 3-11.

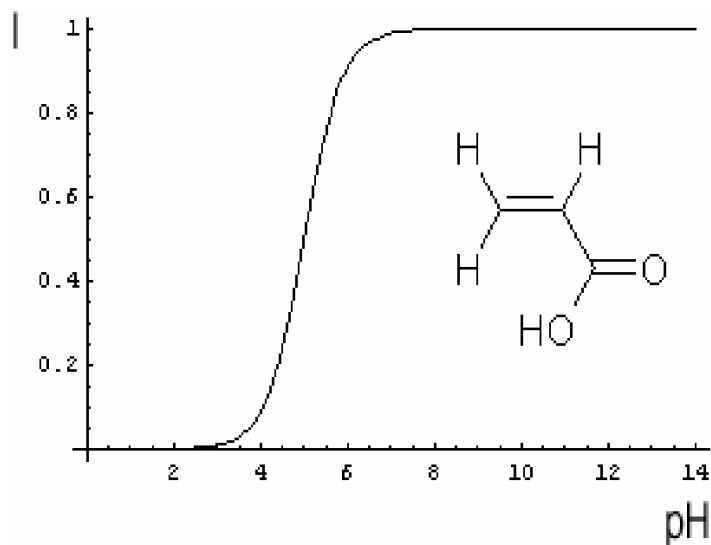


Figure 3-10: Degree of ionization (I) of acrylic acid monomer versus pH [6]

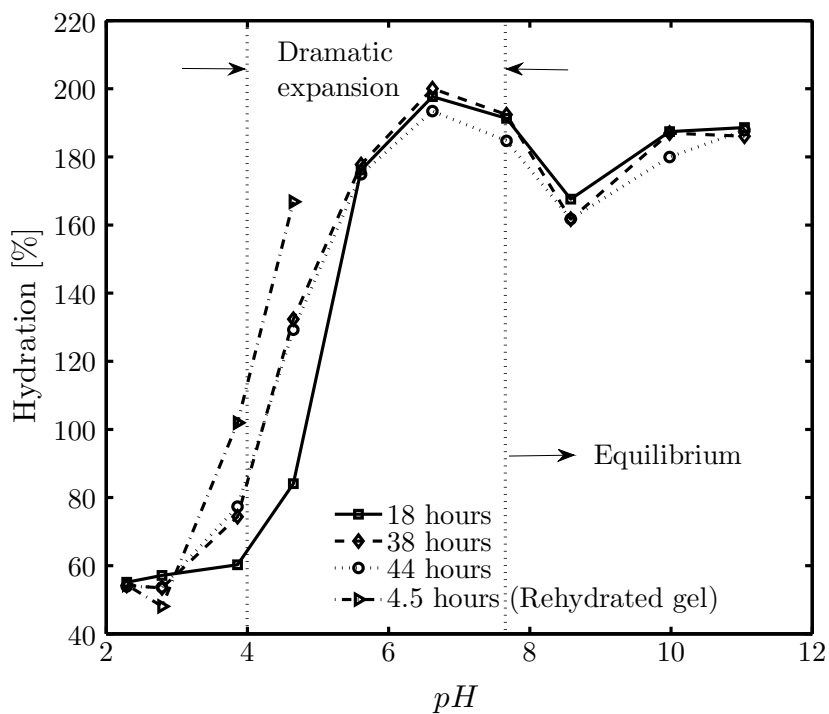


Figure 3-11: Behavior of HEMA-co-AA at equilibrium with the pH buffer

Practical experiments display the trend of HEMA-co-AA as the same as prediction, results of swelling of HEMA-co-AA follow the same trend compared to figure 3-10. Hydrogel expanded much more in pH 4-8 than other pH solutions and get swelling-equilibrium status from $pH > 8$. The pK_a of HEMA-co-AA can be around

Table 3.2: Equilibrium hydration degree of hydrogel in different time interval

Sample	<i>pH</i> buffer	Thickness (μm)	Equilibrium hydration (%)		
			18 hours	38 hours	44 hours
1	2.29	109	55.13	54.20	53.94
2	2.79	114	57.12	53.46	53.66
3	3.86	80	60.25	74.38	77.34
4	4.65	77	84.06	132.35	129.26
5	5.61	80	176.15	177.76	174.90
6	6.62	80	197.68	200.06	193.43
7	7.67	89	191.32	192.41	184.72
8	8.58	67	167.59	161.70	161.75
9	9.98	70	187.41	187.00	179.96
10	11.04	74	188.61	186.06	187.82

5.5-6 which is higher than pK_a of acrylic acid at 4.25. Figure 3-11 also shows a consistent trend for equilibrium status of polymers in different *pH* buffer in different interval of time. At *pH* 8.58, there is a lower expansion compared to others due to the thickness sample used was 67 μm , less than other samples, so the maximum expansion of this sample is lower than others. Regarding to the samples that were dried in air and stored in a nitrogen cabinet for 23 hours and re-hydrated in 4.5 hours, they did not completely behave in the same way as that observed with samples stored in a hydrated phase, because structures of those samples were broken in high *pH* buffer values. Samples should not be stored in dried status but be stored in the appropriate *pH* buffers. Samples should not be stored in dried status but stored in appropriate *pH* buffers. This experiment used different samples for different *pH* value to shorten the time for measurement. This results in a limitation in analyzing the results since the thickness of the samples are not the same. However, the results from this experiment are good for the purpose of observing the behavior trend of HEMA-co-AA as well as predicting the hydration degree of the hydrogel in specific *pH* values. These hydrogel samples demonstrated the expansion compared to the initial volumes (at dry status) of 55-77% at low *pH* 2-4 and expansion of 130-195% at higher *pH* 5-11. Measurements were recorded in different long intervals of time to prove that as soon as the hydrogels reach the equilibrium status, they can no longer expand. The similar

experiment was set up to observe the behavior of the hydrogel but over a shorter time period (not fully equilibrated) when the samples were move from one pH buffer to another for 30 and 60 minutes. The results are presented in figure 3-12.

Over a time period of 30 minutes, the pH range that triggers a strong degree of swelling is between pH 4 and pH 8.5, but when this time period is increased to 60 minutes, this ranges is reduced to below pH 8. This can be explained that in 30 minutes, samples have not got close to the equilibrium, the expansion were not happened completely so the trend of behavior shifted to the right as seen on figure 3-12a. When the measured time is increased, samples got closer to the equilibrium state and the trend moved a little to the left as shown on figure 3-12b.

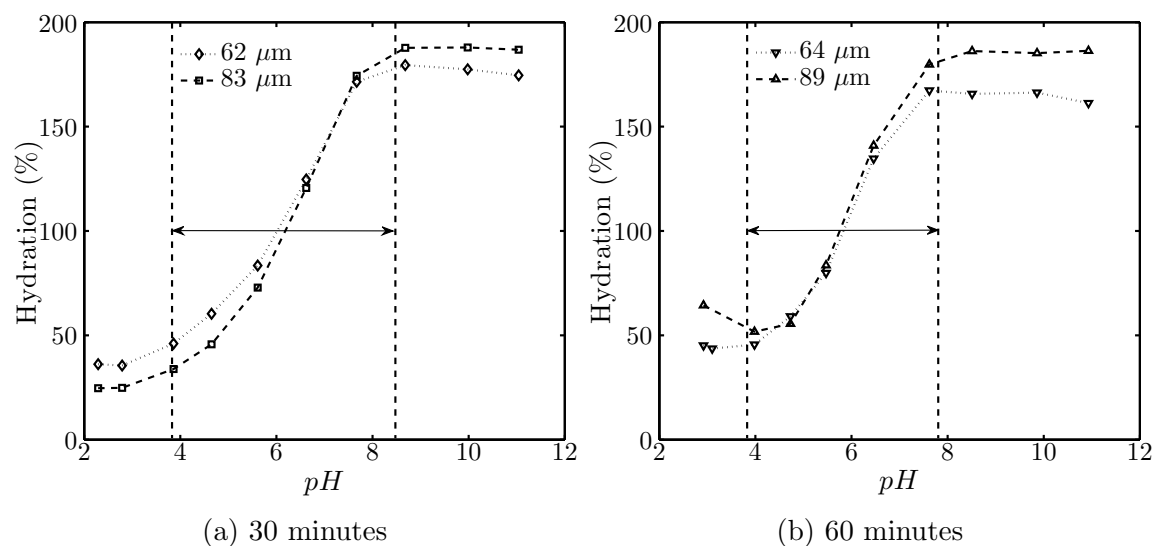


Figure 3-12: Behavior of HEMA-co-AA after exposure to pH buffer in (a) 30 minutes and (b) 60 minutes

3.4.2.4 Behavior of different ratio of HEMA-co-AA

Samples of hydrogel with mole ratio of HEMA:AA 2:1, 4:1, 6:1, samples were moved from pH 2.29 to 11.04 and stayed 30 minutes in each buffer. The sample list was shown in table 3.3. Results show that there are not major differences between these samples as can be seen in figure 3-13. According to the theory about behavior of the hydrogel, the gel with higher comomer ration in its structure (AA) is expected to perform a higher expansion, meaning that HEMA:AA 2:1 is expected with highest

Table 3.3: HEMA-co-AA samples in different ratio

No.	pH buffer	pH buffer	Thickness (μm)
1	2:1	2.29-11.04	61
2	4:1	2.29-11.04	62
3	6:1	2.29-11.04	99

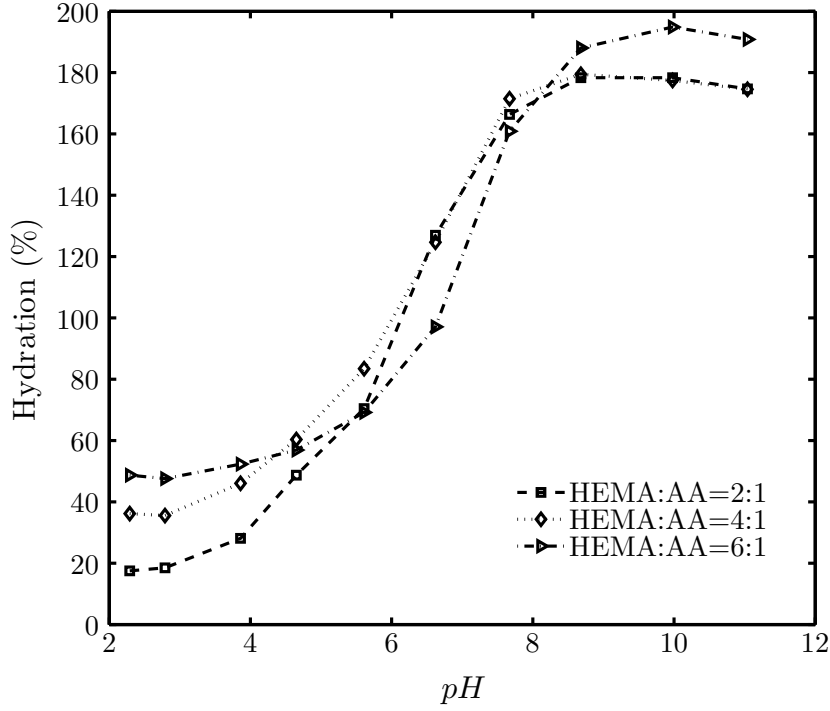


Figure 3-13: Behavior of different ratio of HEMA-co-AA

expansion and HEMA:AA 6:1 with lowest expansion. However, from experimental results, it seems that the change in ratio of HEMA and AA does not affect so much on the degree of hydration in these experiments. This may happen due to the fact that these results were recorded in shorter time compared to the equilibrium time of hydrogel. Therefore, not clear differences between these hydrogels to be observed. In addition, in this experiment, due to the use of different thickness samples, the hydrogel HEMA:AA 6:1 which was thicker than others demonstrated a higher expansion than others.

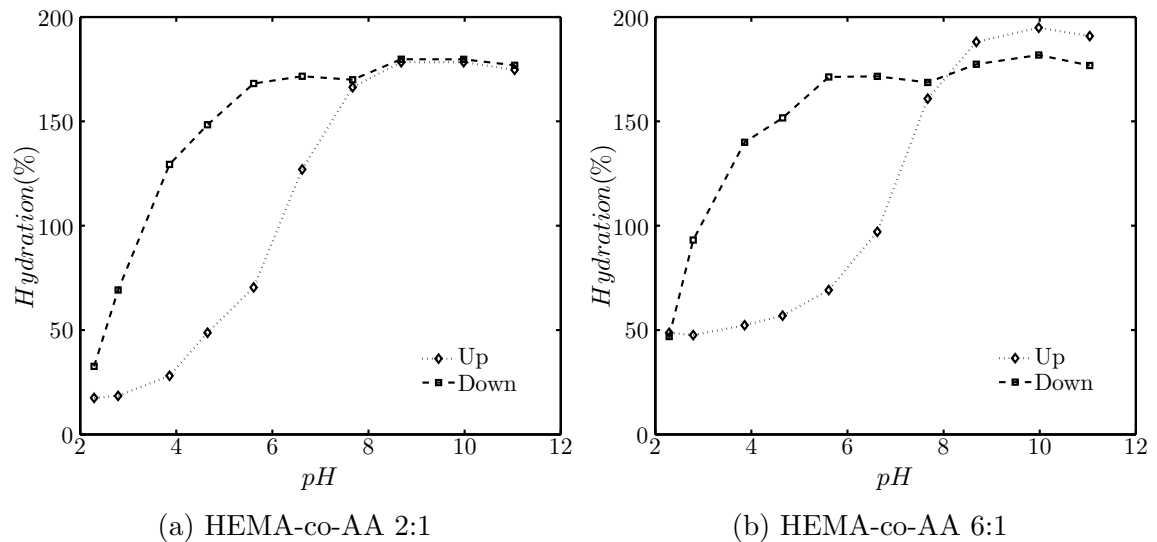


Figure 3-14: Hysteresis of HEMA-co-AA 2:1 in 30 minutes (a) and 6:1 (b)

3.4.2.5 Hysteresis in the behavior of HEMA-co-AA

A hysteresis in behavior of different ratio of HEMA-co-AA has been recorded when samples were immersed in pH solution in 30 minutes. Figure 3-14 shows hysteresis of HEMA-co-AA 2:1 (a) and 6:1 (b).

Hysteresis in response to hydrogel when increasing/decreasing pH shows that for a certain time (lower than time to get equilibrium), there is a delay in the signal when going downstream, meaning that in certain interval of time before the equilibrium status, the expansion of the hydrogel occurs faster than shrinkage. This can be explained by the diffusion time of ions inward and outward of the gel structure. The decrease in volume of the hydrogel when reducing pH is the result of the decrease of osmotic pressure. The protonation of acid groups (precondition) and the moving out of conjugated cations toward solution happen. Therefore, hysteresis in swelling and shrinking of hydrogel can be caused by a delay of deprotonation and protonation, or there is a difference in concentration of H^+ inside the gel at same pH value of solvent.

Looking into the protonation and deprotonation of functional group ($-COOH$) of the hydrogel (equation (2.1)), these two processes are reversible and happened at the same time. However, at non-equilibrium status, the domination of one of two processes will determine the direction of the reaction: $-COOH \rightleftharpoons COO^- + H^+$.

Forward reaction rate r_f and reverse reaction rate r_r of equation (2.1) can be given by basic rate laws

$$r_f = k_f[COOH] \quad (3.15)$$

$$r_r = k_r[COO^-][H^+] \quad (3.16)$$

Since this is a reversible process, rate of reaction (2.1) will be

$$r = r_f - r_r = k_f[COOH] - k_r[COO^-][H^+] \quad (3.17)$$

where k_f is the forward rate coefficient and k_r . These coefficient play a part in the rate of reaction. They depends on temperature, ionic strength, absorbent surface, catalyst, etc which affect the chemical reaction. We assume that temperature and ionic strength is constant in these experiments. The absorbent surface may be a cause for the difference of protonation and deprotonation rate. When the gel is on the way to expand (increasing pH), the surface on hydrogel sample is broadened and oppositely to shrinking gel (decreasing pH), the surface is diminished. Therefore, the protonation (decreasing pH) is lower than the deprotonation (increasing pH). Other reasons due to the complicated kinetic of hydrogel behavior can also happened.

Hysteresis of hydrogel is an important issue when incorporating it into transducer. If swelling degree of the hydrogel depends on the direction of pH change, it cannot be usable for the sensor. However, we can avoid hysteresis by measuring at equilibrium status, means $r = r_f - r_r = 0$. To reduce the equilibrium time of the hydrogel, thickness should be reduced.

As can be seen in figure 3-15, hysteresis between upstream and downstream of the hydrogel stayed in solution in 60 minutes (figure 3-15a) is smaller than that of hydrogel stayed in solution in 30 minutes (figure 3-15b). That means the closer the recording time for measurement to the equilibrium status, the less hysteresis is. In addition, it can be seen that hysteresis mostly happened below pH 8 for the reason that the hydrogel obtained the maximum volume at this pH . Hysteresis of hydrogel

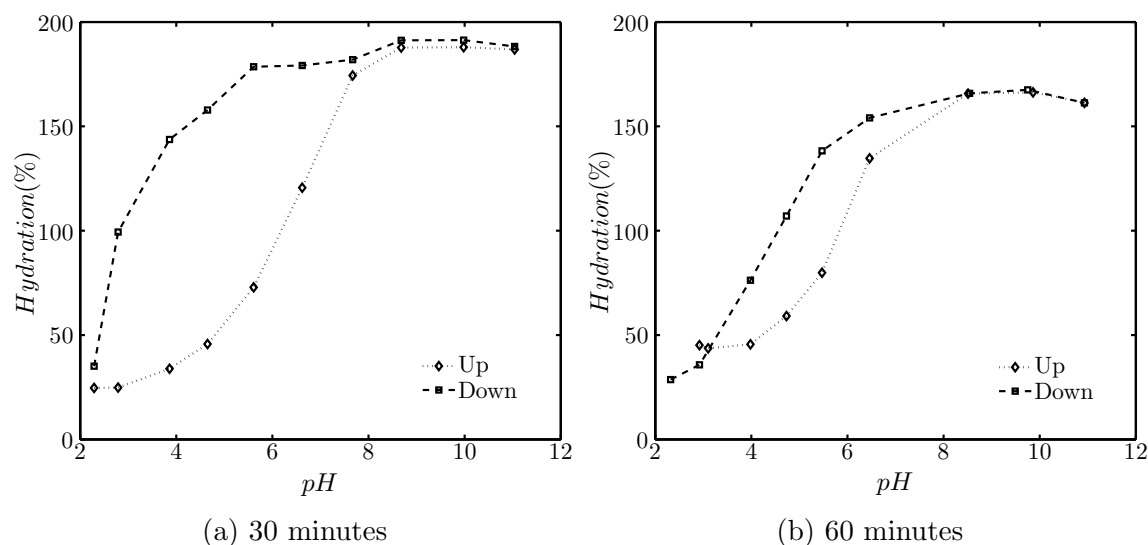


Figure 3-15: Hysteresis of HEMA-co-AA 4:1 in 30 minutes (a) and 60 minutes (b)

is also reported in a review of Gerlach et al [14] but does not explain clearly for this phenomenon.

3.5 Conclusions

The experimental results show that the profilometer can be used to characterize hydrogel behavior. The hydrogel samples with thickness from 77-110 μm performed the expansion degree of 55-77% at low pH 2-4 and of 130-195% at higher pH 5-11. Both the equilibrium time and the maximum expansion of hydrogel samples were influenced by their thickness. pK_a of hydrogel HEMA-co-AA is approximately 5.5-6, higher than that of acrylic acid. The hydration degree of HEMA-AA polymer can be predicted at specific pH . In addition, hydrogel should be stored in appropriate buffer (after hydrating for the first time) to avoid any damage to the structure. The mechanical changes in the polymer experience a hysteresis when subject to a rising pH compared to a reduced pH . This can be explained by a delay of protonation compared to protonation process. This hysteresis can be minimized by increasing the reaction time of the hydrogel in solution. The results show that HEMA-co-AA is suitable to be integrated in a pH sensor to measure pH in the range of 4-8. This range is also relevant for pH changes inside the human body (pH 6.6-pH 7.4), which

means that it is possible to make sensors that incorporates HEMA-co-AA for work tailored measurements in living tissue.

Chapter 4

Hydrogel based biosensor

This chapter follows the work performed in chapter 3 in which the HEMA-co-AA 4:1 is integrated together with the silicon pressure sensor to construct a hydrogel sensor. The aim is to test the sensor within the same pH range 4-8 which was the range in which the hydrogel had its most dramatic change in volume. This chapter starts with an introduction about the general working principle of hydrogel sensors as well as specific working principle for hydrogel sensors based on piezoresistive pressure sensor. The chapter also shows some previous designs of pH -sensitive hydrogel sensors and an explanation for ability of generating pressure of the hydrogel inside the constraint volume of a pressure sensor's cavity. The experimental works describes the design, assembly-packaging and the measurement methods used to characterize the hydrogel sensor and completes with the results and discussions part.

4.1 Introduction

4.1.1 Hydrogel based sensor

A hydrogel based sensor (or a hydrogel sensor) consist of two main components in their structure: (i) sensing element hydrogel and (ii) a transducer. The hydrogel plays the role as the sensing element that converts a specific stimuli in the surrounding environment to changes of volume. The transducer will convert the physical signals

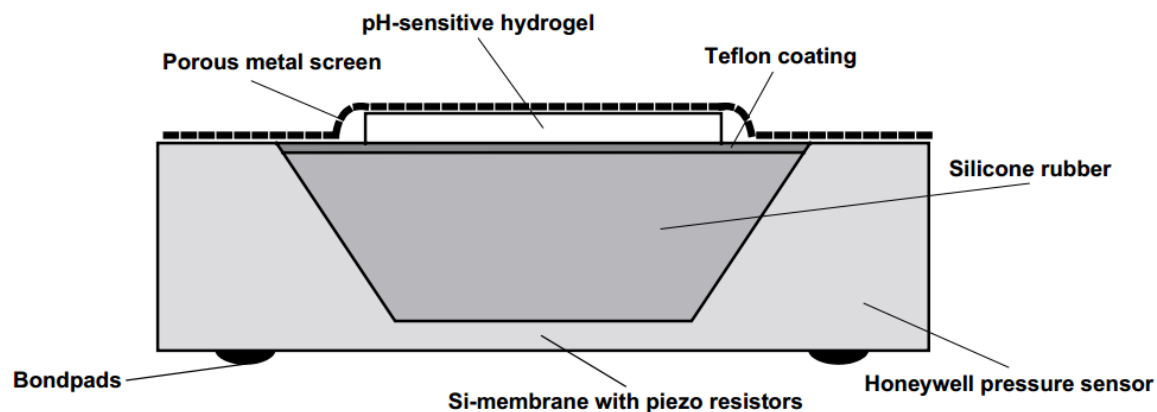


Figure 4-1: A design from Herber et al (2004) [37] for CO₂ sensor based on piezoresistive pressure sensor

occurring from changes in the hydrogel volume to a specific electrical signal that can be read out by an associated electronic circuit (or instrument).

Principles of hydrogel sensors

A review on hydrogel-based pH sensors and microactuators were made by Richer et al (2008) [32]. According to Richer, hydrogel sensors can be categorized into two types based on their working principles. The first category is for sensors based on observing changes in properties of free swelling hydrogel. The second category is for sensors based on mechanical work performed by the hydrogel swelling or shrinking. With respect to sensors using free swelling gel, they have to observe one or more properties of the hydrogel. They can be optical transducers that measure changes in optical properties of hydrogels such as transmission (shrunken state hydrogel has lower transmission coefficient while swollen state hydrogel is usually transparent high transmission coefficient), refractive index (swollen gel has lower refractive index than that of shrunken gel), reflection (reflection intensity decreases as gel swells), optical wavelength diffraction (change in hydrogel volume shifts the diffraction to longer wavelength), or labeling hydrogel with fluorophore and observing a change of fluorescence intensity (swollen gel has lower intensity than shrunken gel). They can be conductometric transducers in which hydrogel layer is coated on electrode array, and where the swelling of the hydrogel layer results in an increase in the conductance, accompanied by a decrease in resistance). They can be oscillating transducers which

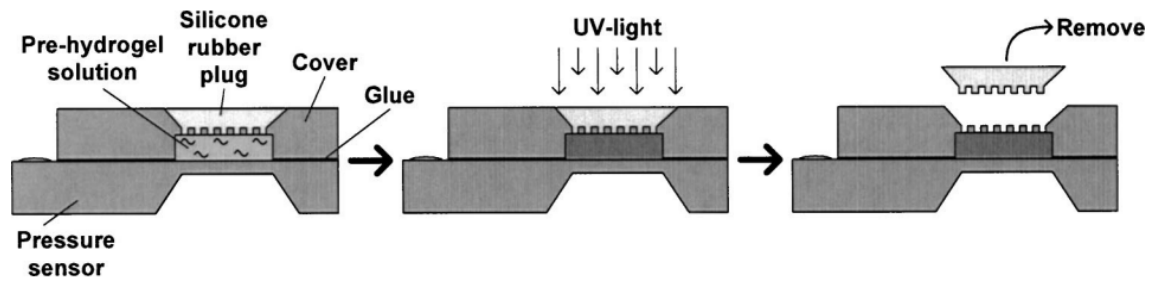


Figure 4-2: A design from Herber et al (2004) [38] for CO₂ sensor based on piezoresistive pressure sensor

the changes in the mass of hydrogel (due to swelling or shrinking) will convert to a shift in the resonance frequency. Some kinds of oscillating transducers which can be mentioned are quartz crystal micro balance (QCM) and magnetoelastic sensors.

For the second category of transducers based on mechanical work exerted by the hydrogel, the swelling or shrinking action of hydrogel will cause deformation on the transduction element resulting in a change in specific property of that element or a change of detectable distance. They can be optical transducers with reflective diaphragms (hydrogel is coupled to a reflector, when hydrogel changes its volume, it makes diaphragm to move, as a result, intensity of light reflected back into the optical fibre changes). Other type is fibre BRAGG grating sensor which based on fibre optic BRAGG grating sensors (swollen gel increase the BRAGG wavelength and shrunk hydrogel reduces BRAGG wavelength). Mechanical transducers such as microcantilevers which can transduce a change of mass, temperature, heat or stress into a bending action or to a change in resonance frequency also belong to this category. Microcantilevers are usually coupled with an optical or piezoresistive readout system.

A bending plate transducer is another kind of mechanical transducer which usually includes a piezo-resistive Wheatstone bridge (for example a pressure sensor). A hydrogel element is incorporated into this kind of sensor in confined conditions, where a change in the volume of the hydrogel will deflect the plate and resulting in change in resistance of the bridge.

Designs of hydrogel sensors based on piezoresistive pressure sensor

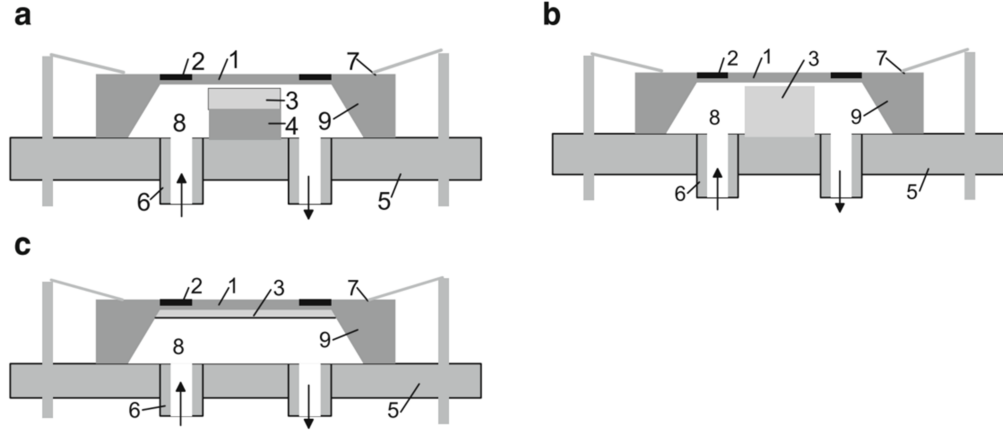


Figure 4-3: Designs from Gerlach and Guenther [39] 1 bending plate, 2 mechano-electrical transducer (piezoresistive bridge), 3 swellable hydrogel, 4 Si substrate (5x5x0.3 mm³), 5 socket, 6 tube, 7 interconnect, 8 solution, 9 Si chip (5x5x0.4 mm³). 50-100 μm dry hydrogel on a silicon flatform (a), 50 μm dry hydrogel piece was glued to the socket (b), 4-50 μm hydrogel layer was deposited on the backside of the membrane (c)

Several attempts of making such a piezoresistive hydrogel sensor have been made before. S. Herber et al (2004) [37] presented a fabricated hydrogel sensor by filling the cavity of the pressure sensor with silicone and placing hydrogel disk on top and afterward the gel disk was covered by porous metal screen (figure 4-1). Later his group fabricated another sensor with a porous cover to hold the gel inside. The gel was in a direct contact with the silicon membrane of the sensor, and the hydrogel was injected and in situ synthesized. These fabricated sensor designs helped to control the expected thickness of the hydrogel by controlling the cavity depth of the porous cover (5 and 10 μm). Therefore the response time for the sensor could be kept short (figure 4-2). Gerlach and Guenther has also presented some designs in their review on hydrogel sensors and actuators [39] (figure 4-3). Gerlach et al [16] provided another design for using PNIPAAm (N-Isopropylacrylamides) hydrogel (figure 4-4).

$$\Delta\Pi = \Delta\Pi_{\text{mix}} + \Delta\Pi_{\text{el}} + \Delta\Pi_{\text{ion}} = \Delta\Pi_{\text{el}} + \Delta\Pi_{\text{ion}} \quad (4.1)$$

Generation pressure of hydrogels under isochoric condition

All the above designs have one thing in common which is that the hydrogel should

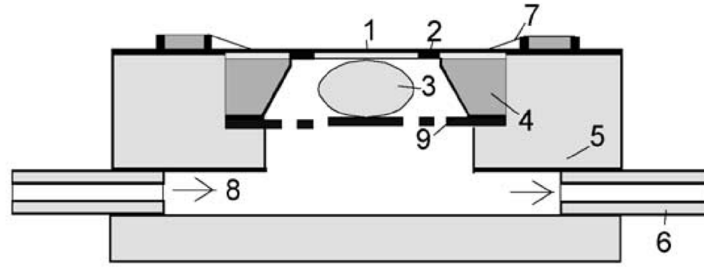


Figure 4-4: Design from Gerlach et al [16] 1 bending plate, 2 mechano-electrical transducer (piezoresistive bridge), 3 swellable hydrogel, 4 Si-chip, 5 socket, 6 tube, 7 interconnect, 8 solution, 9 grate

be confined in all directions but have and has to be in contact with the stimulus in the surrounding solution by a porous membrane. A study for the ability of hydrogel to generate pressure under isochoric conditions was presented by Herber et al [38]. In this study, DMAEMA-co-HEMA hydrogel with thickness $15 \mu\text{m}$ was used to induce a pressure of 67 kPa in 12 min for each step of pH from 9 to 6. The results from this research demonstrates how pressure can be generated by a hydrogel under isochoric conditions. Under the isochoric condition (constant volume), the total energy of the hydrogel as mentioned in equation (2.2), (2.3) of chapter 2 can be rewritten by equation (4.1). In this case, where $\Delta\Pi_{\text{mix}}$ assumed to be zero (when hydrogel get expansion to the same volume of the cavity, and water flow cannot go in or out of the hydrogel anymore) and $\Delta\Pi_{\text{el}}$ remains constant because the expansion of the gel cannot happen in the isochoric condition. Therefore the osmotic pressure is the main factor for ability of the gel to expand and generate ion of a pressure of swollen hydrogel inside the cavity and toward the silicon membrane.

4.1.2 Working principle of pH-hydrogel based sensor

This section introduces the working principle of a hydrogel based sensor based on a piezoresistive pressure sensor. The piezoresistive effect is a change in the electrical resistivity of a metal or a semiconductor when mechanical strain is applied. Especially, this effect is more significant in semiconductor material such as silicon. A relationship between resistance and strain for a piezo resistor element can be presented by equation

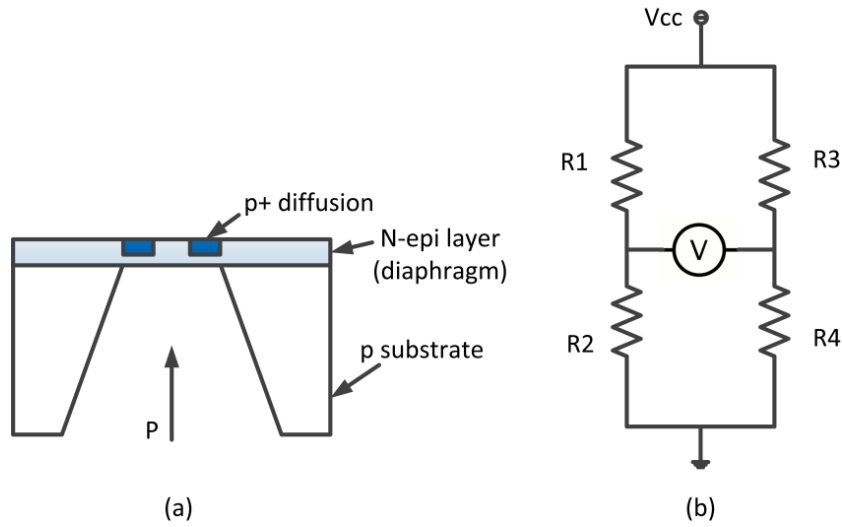


Figure 4-5: (a) Silicon pressure sensor, (b) Wheatstone bridge circuit.

(4.2) [14], where ΔR is the change of resistance, R_0 the unstrained resistance of the piezo resistor, G the gauge factor given by equation (4.3), ν is the Poisson's ratio, e the strain, and ρ the resistivity. The term $(1/e)(\Delta\rho/\rho)$ which is representing the strain-induced changes in resistivity can be large, depending on the gauge factor. The result is a large change in resistance according to (4.2). Silicon material which have been lightly doped can have a gauge factor between +100 and +175 for p-type silicon and between -100 and -140 for n-type silicon (a negative factor means a decrease in resistance for an increased tensile strain).

$$\frac{\Delta R}{R_0} = Ge \quad (4.2)$$

$$G = 1 + 2\nu + \frac{1}{e} \frac{\Delta\rho}{\rho} \quad (4.3)$$

In piezoresistive pressure sensors, the elastic element consists of a flat silicon diaphragm. The distortion of the diaphragm is sensed by four piezoresistive strain elements made by introducing piezoresistors in the areas of the silicon diaphragm, where the strain is the greatest [14]. On the silicon diaphragm, four piezoresistive elements (two in tension, two in compression) are incorporated into a bridge circuit (figure 4-5). The difference in output voltage U_{out} of the Wheatstone bridge is calculated according to equation (4.4) where R_1 , R_2 , R_3 , R_4 is the resistance of the

piezoresistive elements and given by $R_1 = R_3 = R_0(1 - Ge)$, $R_2 = R_4 = R_0(1 + Ge)$ and V_{cc} is supplied voltage for the bridge. Since the strain e has a relation to stress according to equation (4.5) and σ is defined by the force/area by equation (4.6), σ can be considered to be equal to pressure P applied to the sensor (in this case a pressure sensor). So considering $\sigma = P$, we can write out the relationship between the output voltage of the bridge as a product between the unrestrained resistance, gauge factor and pressure and the Young's modulus of the silicon diaphragm as shown in (4.7). So theoretically, the output voltage U_{out} from the Wheatstone bridge implanted on silicon diaphragm is a linear function of applied pressure P to the diaphragm.

$$U_{out} = V_{cc} \left(\frac{R_2}{R_1 + R_2} - \frac{R_4}{R_3 + R_4} \right) = R_0 G e \quad (4.4)$$

$$e = \sigma / E \quad (4.5)$$

$$\sigma = \frac{F}{A} = P \quad (4.6)$$

$$U_{out} = R_0 G e = R_0 G P \quad (4.7)$$

where E is the Young's modulus

This applied pressure in a hydrogel based sensor will be generated from the expansion of an integrated hydrogel. The deflection of the diaphragm will change the bridge resistance and generate a change in the output voltage as a function of the applied pressure. The magnitude of the applied pressure and consequently the output voltage will be related to the expansion or shrinkage of the hydrogel, which in turn depends on the pH of the surrounding solution that the hydrogel is exposed to.

4.2 Experimental work

4.2.1 Design of the hydrogel sensor and packaging

The feasible approach in this project isto incorporate the HEMA-co-AA (4:1) hydrogel inside the cavity of a commercial pressure sensor, which was covered by the stainless steel porous membrane. The porous membrane plays the roles to hold the hydrogel in

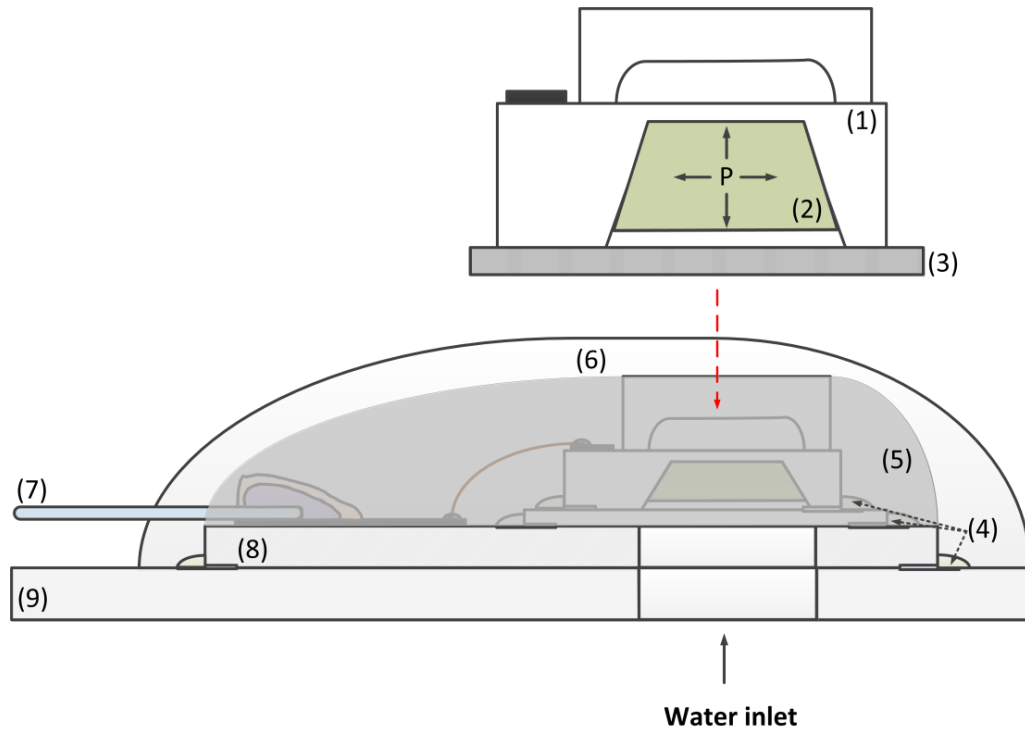


Figure 4-6: The design of hydrogel sensor including (1) piezoresistive pressure sensor, (2) hydrogel HEMA-co-AA (4:1), (3) stainless steel porous membrane, (4) adhesives, (5) glop-top layer, (6) waterproof water layer, (7) electrical wires, (8) chip carrier, (9) PCB

the cavity but still allows the hydrogel to contact with stimuli factors from solution. The sensor will be wire bonded to a chip carrier which designed to have a hole at the center for the inlet of solution. Via this hole the hydrogel inside the cavity can be exposed to the solution and perform its swelling-shrinking. The chip carrier will be connected to external wires for later measuring signals. These components will be placed on a printed circuit board which also has its hole respectively to that on the chip carrier. All the components will be joined together by adhesives. The hydrogel sensor will be covered by glop top material to protect the wire bonds and by the outermost waterproof layer for an electrical insulation when the sensor works in solution. When applying immersing the sensor into pH buffers, the expansion of hydrogel will create a pressure on the membrane of a pressure sensor. Electrical signal can be read out by a read-out platform. The design for the sensor in this project is apparently given in figure 4-6.

MECHANICAL DIMENSIONS (in μm)

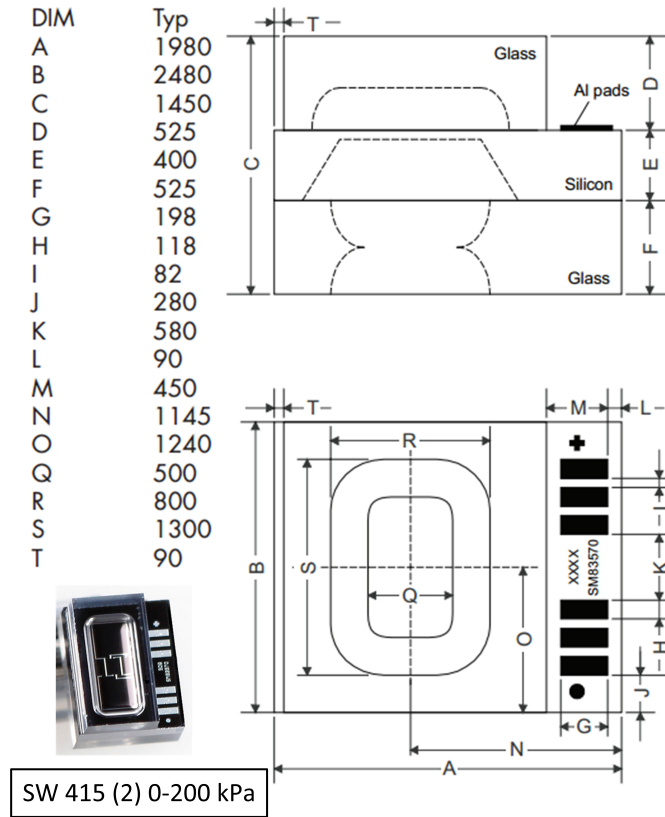


Figure 4-7: Mechanical dimensions (in μm) of the SW415-2 sensor [40]

4.2.2 Materials & Components

Sensor

The silicon piezoresistive pressure sensor (SW415-2, Sensoror, Norway) was used in this project. The silicon die has the dimension of $1980 \times 2480 \times 1450 \mu\text{m}^3$, and has a dynamic range of 0-2 bar absolute pressure. It is bulk micro-machined and designed with buried backside piezoresistive elements making these piezoresistors not exposed to the media that may reside in the etched cavity below the membrane. The SW415-2 sensor has 3 layers of glass (top and bottom layer) and silicon (middle layer) as showed in figure 4-7, the total thickness of the cavity is $925 \mu\text{m}$. Results in chapter 3 indicates that thicker hydrogel gives longer response time, hence, with the purpose to reduce the response time of the hydrogel based sensor by reducing the thickness

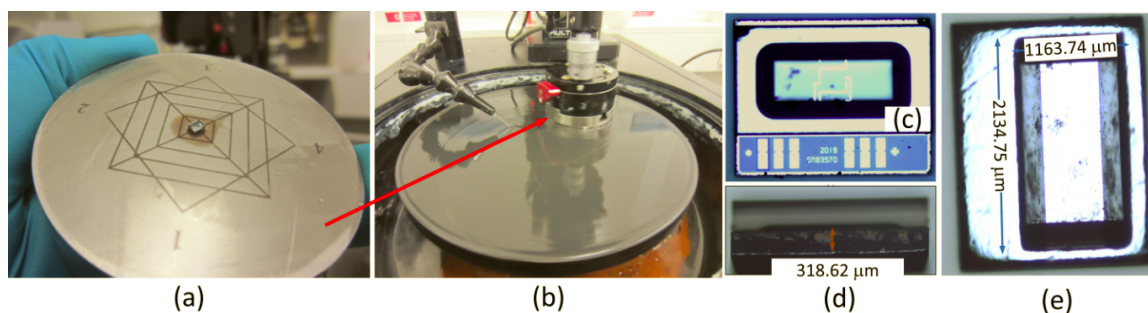


Figure 4-8: The pressure sensor was mounted on fixture (a), which enabled it to be polished by the polisher (b). The modified sensor is shown with the front view (c), side view (d) and back view (f)

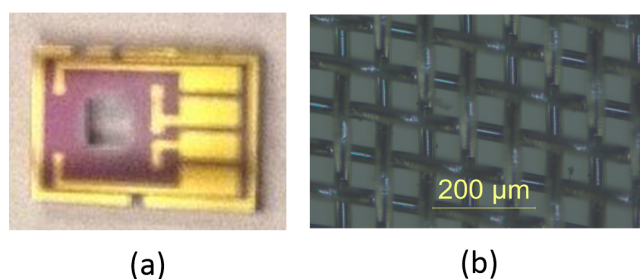


Figure 4-9: Chip carrier (a), Stainless steel membrane (b)

of hydrogel synthesized inside sensor's cavity, the original sensor was polished by a special polishing machine (Multiprep polishing system, Allied High Tech Products Inc., USA) with 320 Grit Silicon Carbide Paper 8 inches (Allied High Tech Products Inc., USA) for raw polishing and with $0.05 \mu\text{m}$ alumina suspension (90-187540, Allied High Tech Products Inc., USA) for fine polishing to remove the bottom layer of glass (Figure 4-8a, b).

The cavity thickness of the sensor after polishing was around $320 \mu\text{m}$ and the opening of the cavity was $2135 \times 1164 \mu\text{m}^2$ compared to $1300 \times 800 \mu\text{m}^2$ when the underlying glass plate was in place. This makes it easier to manually inject the pre-hydrogel mixture into the cavity of the pressure sensor. A view of polished sensor is illustrated in figure 4-8c, d, e.

Substrate (chip holder)

The chip holder was adapted from a substrate used in the Doctorate of Philosophy project of O. Krushinitskaya, Vestfold University College, 2012 [41]. The substrate was fabricated to create a hole in the center which allows the access of pH solution

to the chip. The thin metal film constituting the contact pads on chip holder were made from a 0.5 mm thick layer of gold [41] (figure 4-9a). This component plays a connection role from sensor to external world.

Membrane

A stainless steel membrane #300 mesh, 49 μm in aperture, 36 μm wire diameter (The Mesh Company, United Kingdom) was utilized to hold the polymer inside the sensors cavity. This steel membrane was chosen due to its material properties to be rigid enough to hold the hydrogel inside cavity of sensor and being able to suffer pressure from expansion of hydrogel without significant deformation. On the other hands, it can let water go in and out freely and be stable in low pH buffers (figure 4-9b).

Other chemicals and components

To complete the packaging step of the sensor, some epoxies were used: two components epoxy Araldite 5 min (Huntsman Corporation, Switzerland) to glue membrane to substrate and sensor to membrane; two components silver epoxy (Epotek EE 129-4, USA) to connect contact pads on substrate to external wires, two components glop top epoxy (Epo-tek T7139, USA) to make wire-bonds stronger and protect them; two parts silicone (MED3-4013, NuSil Technology, USA) and one part silicon (Dow Corning 3140 RTV Coating, USA) to form a waterproof outer layer so that the sensor can work long time in solution. pH buffers from pH 2 to 8 were prepared as described in chapter 3. For electrical measurement, a data acquisition card (DAQ) (NI USB 6211, National Instruments, USA) was used for signal acquisition (DAQ), Labview System Design Software 2015 (National Instruments, USA-HBV license) was used to read out the signal on computer, dual-op-amp (OPA2137, Burr Brown, USA). Other electrical components were supported by electronic lab at HBV.

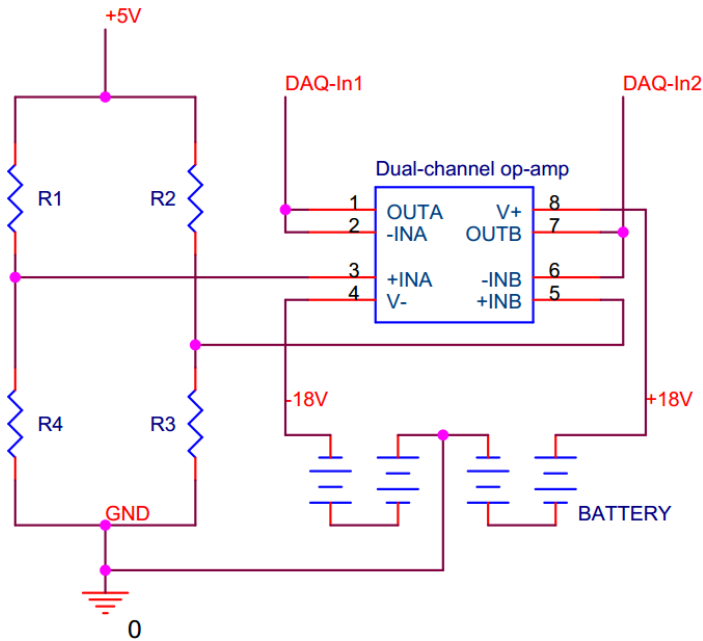


Figure 4-10: Schematic of the signal conditioning circuit for the sensor

4.2.3 Method

4.2.3.1 Experimental setup

In order to measure the signals from sensor, electrical measurement system has been set up. Principle for electrical measurement of the sensor is represented by figure 4-10. Here, a dual-op-amp (operational amplifier) was used as a buffer for the circuit. The sensor was powered by a 5 V DC source, and the op-amp was powered by 4 batteries 9 V. The difference in output signals were connected to DAQ, and then to a computer with Labview software which was written to read out the signal from the DAQ. The Labview program is presented in figure 4-11. The measurement system is illustrated by a flow in figure 4-12. There are 4 experiments to be conducted as listed below.

Experiment 1: Test of the Electrical signal conditioning circuitry

Test 1 was conducted to investigate if the electrical circuit worked properly without the sensor. Two independent DC sources were used to supply 5V directly to each inlet of the dual op-amp. The op-amp was supplied by 18 VDC. The electrical circuit did not consist any sensor. The dual op-amp plays the role as the buffer with gain =

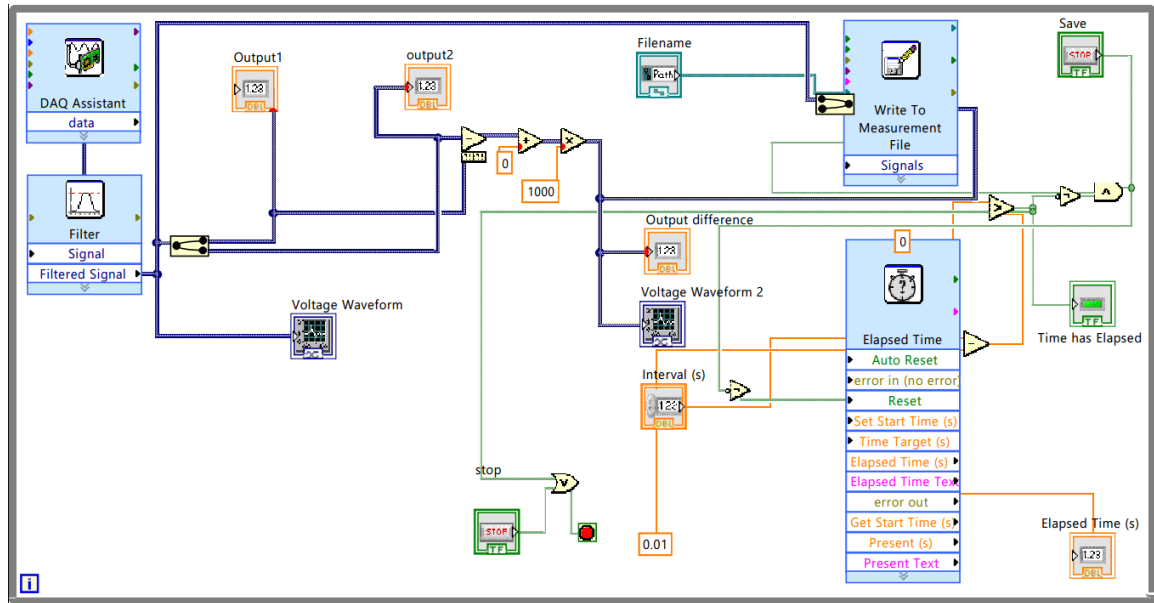


Figure 4-11: Labview program

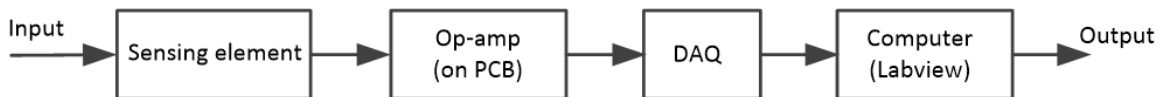


Figure 4-12: Components of the measurement system

1. The expected output signal is the same with supplied voltage.

Experiment 2: Test of SW415-2 pressure sensor

Experiment 2 was to map the signal from original SW415-2 pressure sensor. The sensor was tested at the range of pressure from 0-2 bar (upstream and downstream) with steps of 0.1 bar. The pressure was controlled by a chamber and a pump. The sensor was gold-wire bonded to the chip carrier which already connected to external wires. Several ways of assembling the sensor and interconnect it to the outside world were attempted as shown in figure 4-13: sensor connected directly to PCB by wire-bonding without chip carrier(c), sensor was first wire-bonded to chip carrier, then chip carrier was connected with external wires by headers (a), chip carrier connected with wires by using conductive silver epoxy (b). The direct bonding of sensor to PCB seems to be the most simple way to do. However, before bonding to the PCB, the sensor had to be mounted into a hole drilled on PCB using adhesive. The adhesive was not strong enough to suspend the sensor within the hole, causing some problem

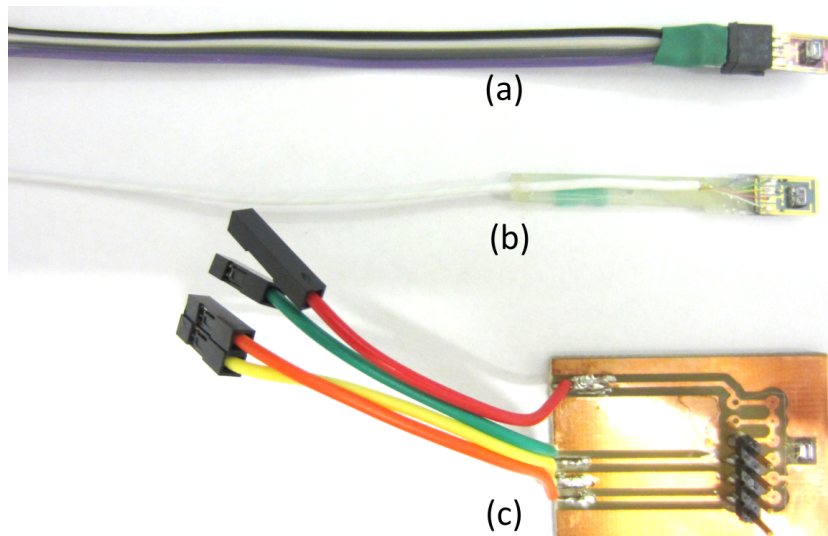


Figure 4-13: Chip carrier connected with external wires by headers (a), chip carrier connected with wires by using conductive silver epoxy (b), sensor connected directly to PCB by wire-bonding



Figure 4-14: Comparison in size of the sensor with a normal pen

with the bonding process. Moreover, for further process to package the sensor, it is necessary to have a substrate to hold the porous membrane adjacent to the sensor. Another reason for not directly bonding to the PCB is the expansion of PCB in water may happen. Silicon membrane does not have this problem. So it is better for the sensor to attach on a chip carrier. Considering (a) and (b), (a) given a easier way to attach the headers on contact pads of chip carrier. But after attaching the headers, the bottom face of chip carrier is not flat and wire bonding can be done. Wire-bonding was decided not to be the first step to avoid breaking of delicate wire bonds during the process of packaging. Only (b) was chosen to be continue for the rest of lab work.

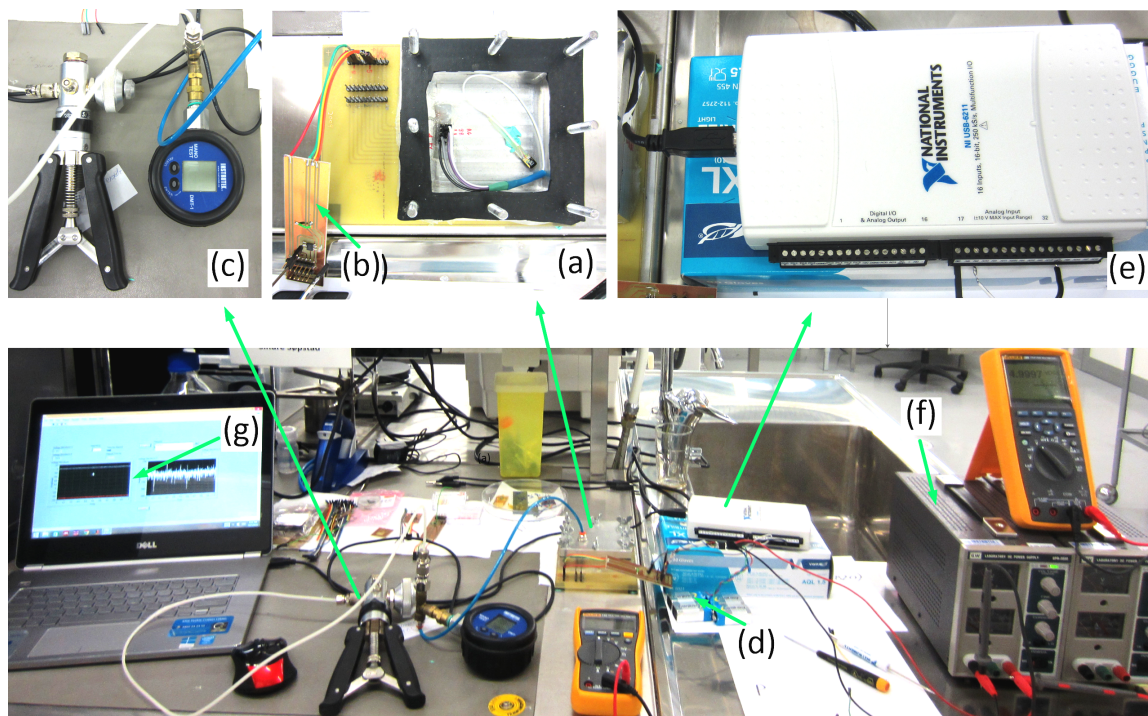


Figure 4-15: (a) Sensor inside chamber, (b) PCB, (c) pump, (d) battery, (e) DAQ, (f) power source, (g) computer with Labview interface

Sensor was checked if the Wheatstone bridge is balance before measuring the signal, meaning that the bridge resistance is around $12\text{ k}\Omega$. The sensor was placed inside a chamber, connecting to the inner pins of the chamber, PCB was connected to the outer pins of the chamber in respect and then to the PCB. An illustration for the measurement system can be seen in figure 4-15 and a comparison of size of sensor to a normal pen can be seen in figure 4-14.

Experiment 3: Test of polished SW415-2 pressure sensor

Experiment 3 was to confirm the the functionality of the sensor after removing the bottom layer of glass. Measurement was set up as similar as experiment 2.

Experiment 4:

Experiment 4 was used to characterize the hydrogel-based sensor. Since the working environment of sensor would be in solution, so the sensor must go through a packaging procedure as described in detail in section 4.2.3.2. After packaging, sensor was immersed in the solution (figure 4-16). Sensor was first dipped in pH buffer 2.39 (25°C) for completed hydration process before moving to the next higher pH buffers.

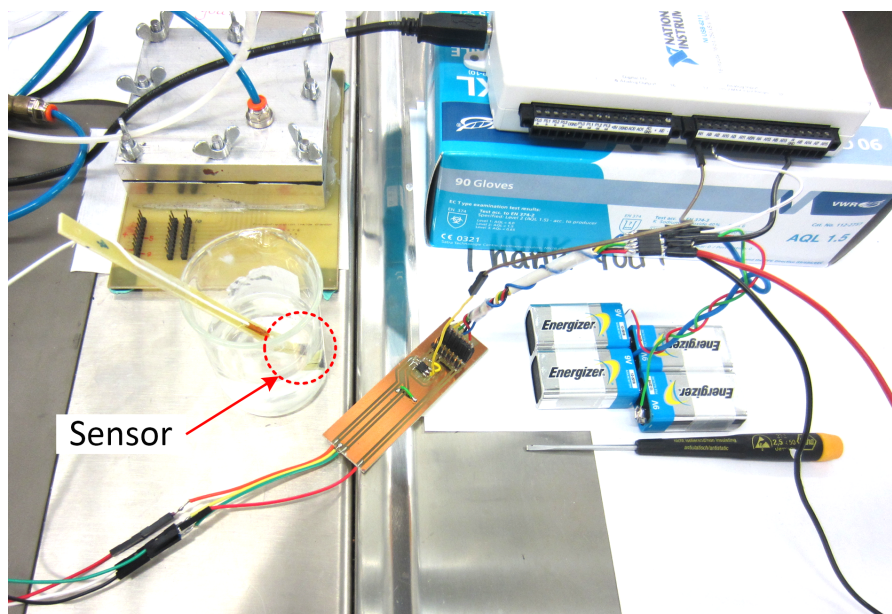


Figure 4-16: Sensor in pH buffer

The system was covered by plastic film to avoid the solution from evaporating.

4.2.3.2 Sensor assembly procedure

The packaging process is summarized by figure 4-17, and most of steps were done under a microscope. Packaging is one of the most important steps to get the signals from sensor system. SW415-2 was first polished to remove the bottom layer before the hydrogel HEMA-co-AA (4:1) was in situ synthesized inside its cavity (figure 4-17a, b, c). The pre-hydrogel solution was injected to the backside cavity of the sensor by using micropipette and cured under UV light with the same conditions described in chapter 3. The synthesized hydrogels had the thickness around $200\ \mu\text{m}$ compared to thickness of the polished sensors cavity around $300\ \mu\text{m}$ (thickness determined by the microscope (Gendersew and Loken Instrumenter AS, Norway)). According to results from chapter 3, the expected expansion degree of these hydrogels with this thickness will be more than 55% with $pH > 2$. This allow the achievement of signals when immersing the sensor to the pH buffers > 7 .

The chip carrier with contact pads (figure 4-17d) was prepared before incorporating with the sensor via gold wire bonds. The chip carrier was glued with electrical

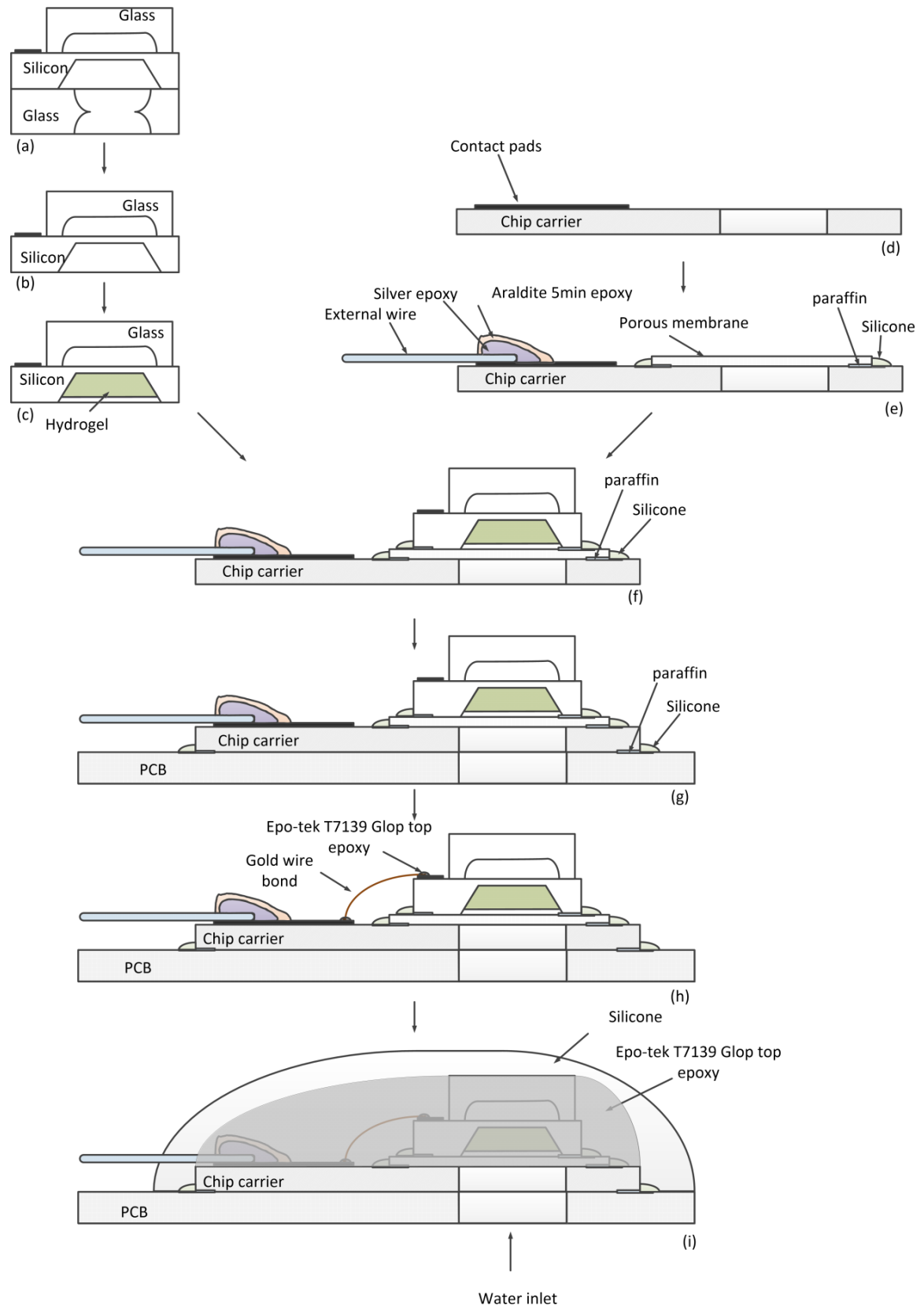


Figure 4-17: A schematic diagram showing the sequential steps of assembling the sensor

wires on its gold contact pads by the conductive silver epoxy and then covered by a layer of two components epoxy (Araldite 5 min) to harden the bonds. Stainless steel porous membrane was also glue upon the hole of the chip carrier (figure 4-17e). Pressure sensor with integrated hydrogel was stuck to the chip carrier and then to the PCB, the gold wire bonds were bonded from the contact pads on sensor to those of the chip carrier. Foot of each wire bond was covered by the epoxy before the whole area to be encapsulated inside the glop top epoxy to protect all wire bonds. Silicone was dispersed as the outer layer to make the whole system waterproof. There are some different points in the packaging steps that have been attempted, mainly about the types of chemicals (glue) utilized for joining sensor-membrane, membrane-substrate, substrate-PCB, and type of silicon for outer waterproof layer. Each procedure was conducted by individual sensors.

Procedure 1: Araldite 5 min (Huntsman Corporation, Switzerland) was applied to link sensor-membrane, membrane-substrate, substrate-PCB cured for 2 hours at 80°C. Two parts silicone MED3-4013 (NuSil Technology, USA) was used to make a cover layer, cured at 50°C for one hour and at room temperature for a day.

Procedure 2: Araldite 5 min (Huntsman Corporation, Switzerland) was applied to link sensor-membrane, membrane-substrate, substrate-PCB. One part silicon Dow Corning 3140 RTV Coating (USA) was used to make outer layer, cured at room temperature for one day.

Procedure 3: Paraffin wax and silicone (one part silicon Do w Corning 3140 RTV Coating (USA)) was used to glue sensor-membrane, membrane-substrate, substrate-PCB. One part silicon Dow Corning 3140 RTV Coating (USA) was used to make outer layer, cure at roomtemperature. Both paraffin wax and silicone is waterproof and does not to expand in water.

4.3 Result and Discussion

Test 1

The input voltage 5V went directly through each inlet of the dual op-amp on

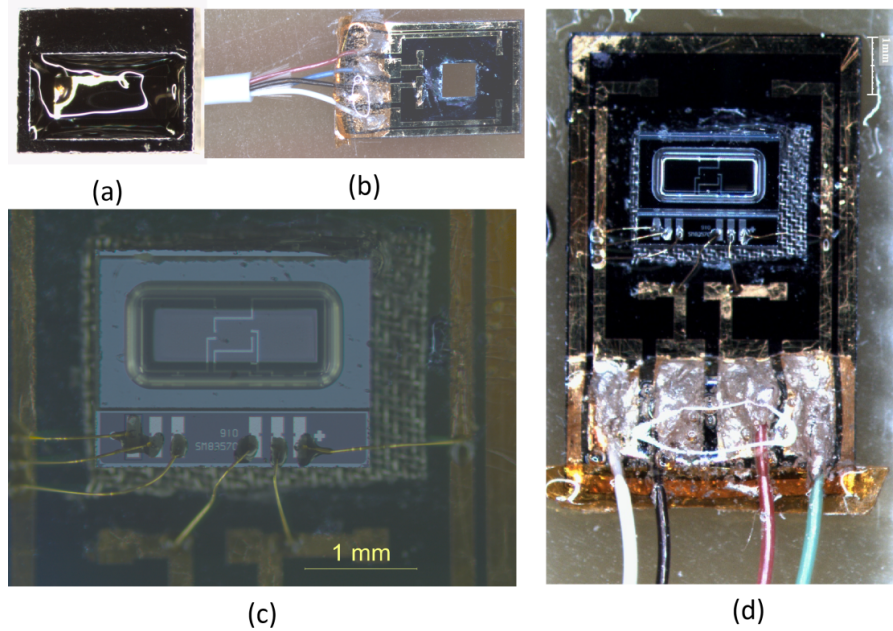


Figure 4-18: (a) The backside of pressure sensor showing synthesized hydrogel inside the cavity, (b) the chip carrier (substrate) was connected to external wires by silver epoxy and Araldite 5 min epoxy on top to strengthen the connection, pressure sensor (with hydrogel inside) with a porous membrane was gold wire-bonded to contact pads on chip carrier (c), a general look of sensor before covered by glop-top epoxy and silicone to be waterproof inside solution (d)

the PCB and read out by Labview on computer with the same value, proving the electrical circuit was working well.

Test 2

Figure 4-19 illustrates response of pressure sensor to change of pressure from 0 to 2 bar. Regression equation for upstream signal is $y = 56.948x - 1.7425$ with coefficient of determination (R squared) $R^2=0.9999$; regression equation for downstream signal is $y = 57.482x - 1.9545$ with $R^2=0.9996$. R squared indicates how well data fit to the regression equation, a R_2 close to 1 indicates that the line perfectly fits to the data. The figure shows that SW415-2 responded very well to the pressure in its working range 0-2 bar.

Test 3 Figure 4-20 presents response of SW415-2 which has been polished to remove the bottom layer. Regression equation for upstream signal is $y = 58.408x + 27.617$ with coefficient of determination (R squared) $R^2=0.9997$; regression equation for downstream signal is $y = 59.43x + 27.289$ with $R^2=0.9999$. Comparison between

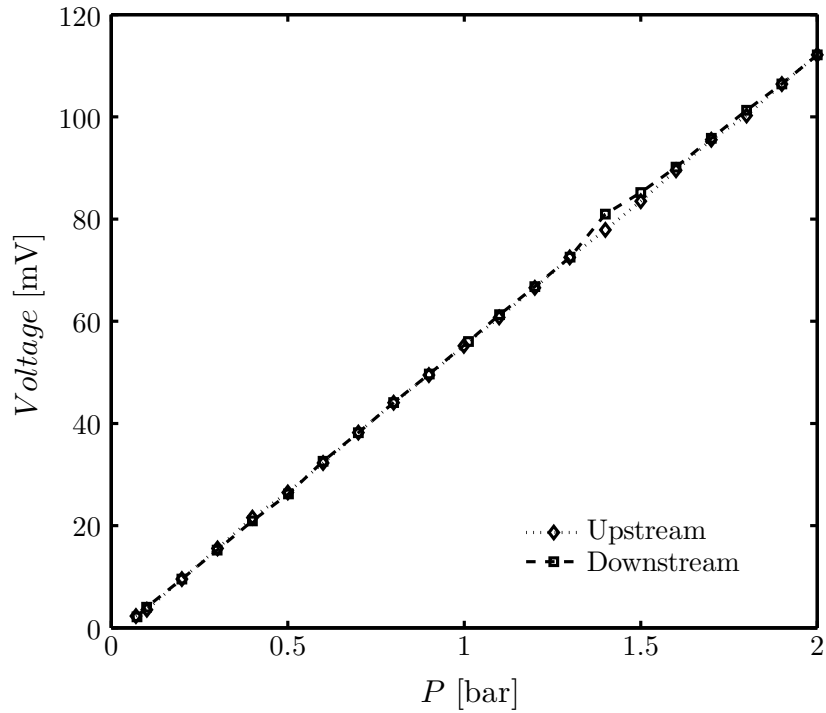


Figure 4-19: Response of SW415-2 pressure sensor to 0-2 bar pressure

regression equations of SW512-2 pressure sensor (figure 4-19) and modified sensor (figure 4-20) shows that the behavior of modified sensor were similar to the original sensor, therefore we can used these polished sensor for the purpose of making pH -sensitive hydrogel based sensor.

Test 4

Procedure 1:

The starting signal was negative, meaning that the silicon diaphragm of the sensor may have been physically pulled down, since the equilibrium position of the membrane is measured against vacuum or zero pressure (figure 4-21). An observation was made between before and after applying silicone showed that the negative signals came after the silicone cured at 50°C. So silicone when shrunk (after cured) may have caused the silicon membrane to go down, giving out the negative signals. This problem was solved when using another kind of silicone (one component silicone Dow Corning 3140 RTV Coating in procedure 2 with less negative signal (around -3 mV compared to -65 mV in this case). The negative signal may have resulted from the shrinking

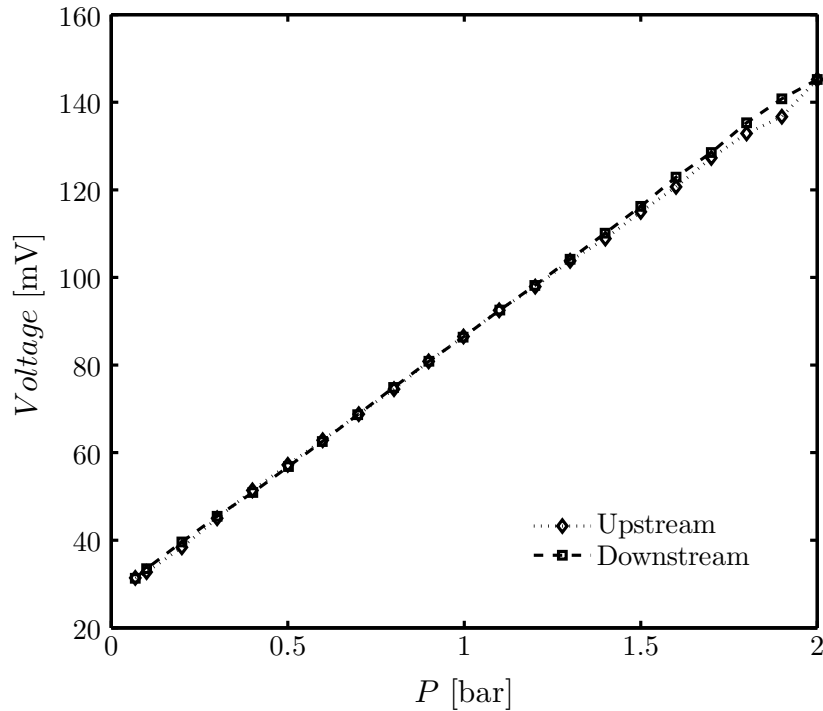


Figure 4-20: Response of polished sensor to 0-2 bar pressure

after curing by UV light of the hydrogel synthesized into the backside cavity of the pressure sensor. In figure 4-21, when sensor was immersed in the pH buffer of 2.31, it got the signal from the expansion of the hydrogel, causing a deformation on the silicon membrane that in turn changed the resistance of the piezoresistive elements, and hence changed the voltage of the output signal. The sensor got in an equilibrium state after 7 hours and stayed in that state for several hours more before the signal started to drastically fluctuate due to some unknown problems.

Procedure 2:

In this test, the type of silicone used in procedure 1 was replaced by one component silicone Dow Corning 3140 RTV Coating (USA) which cured at room temperature for one day. As seen in figure 4-22 the starting signal was a bit negative, showing that this type of silicone when cured did not create much stress on silicon membrane. Signals from sensor go up proved that it got the signal from the expansion of hydrogel inside the cavity and got equilibrium around 7 hours. Afterward, expected signal should have been stable at the equilibrium state but in reality, the signal did go up to very

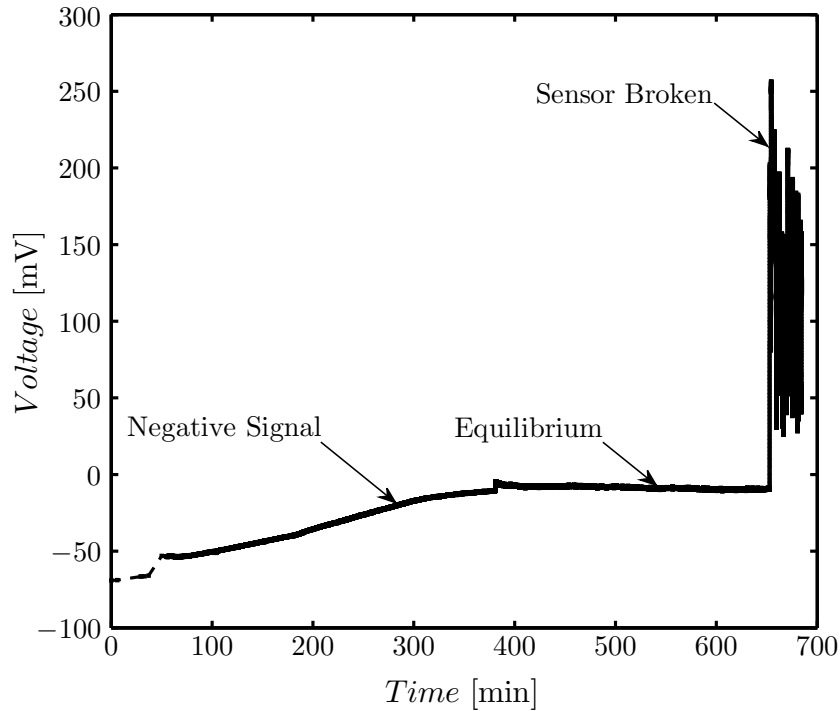


Figure 4-21: Hydrogel-based sensor of procedure 1 in pH 2.34

high of voltage and continue increasing after sensor was taken out of the solution for several hours more before decreasing (up to a equivalent pressure of 5 bar).

Sensors was taken out of the water to check the balance of Wheatstone bridge and observed under microscope, showing that the hydrogel was still within the cavity covered by porous membrane and silicon membrane of pressure sensor remained to work well (figure 4-23), proving that the steel stainless membrane can hold the hydrogel inside.

Comparison between signals in figure 4-24 shows that at the first period, both sensors got the signal of expansion from hydrogel, resulting in increases in voltage, proving that hydrogel sensors did work well to convert signal from swelling of hydrogel to electrical signal. After expansion, two sensors got in equilibrium after approximately 7 hours. The data was reasonable because gel synthesized in cavity of those sensor were around $200\ \mu\text{m}$ then having the longer response time compared to that of thinner hydrogel investigating in chapter 3. Compared to experiment in section 3.4.2.2 and refer to equation 3.14 (and assume that the data generate by hydrogel sensor is cor-

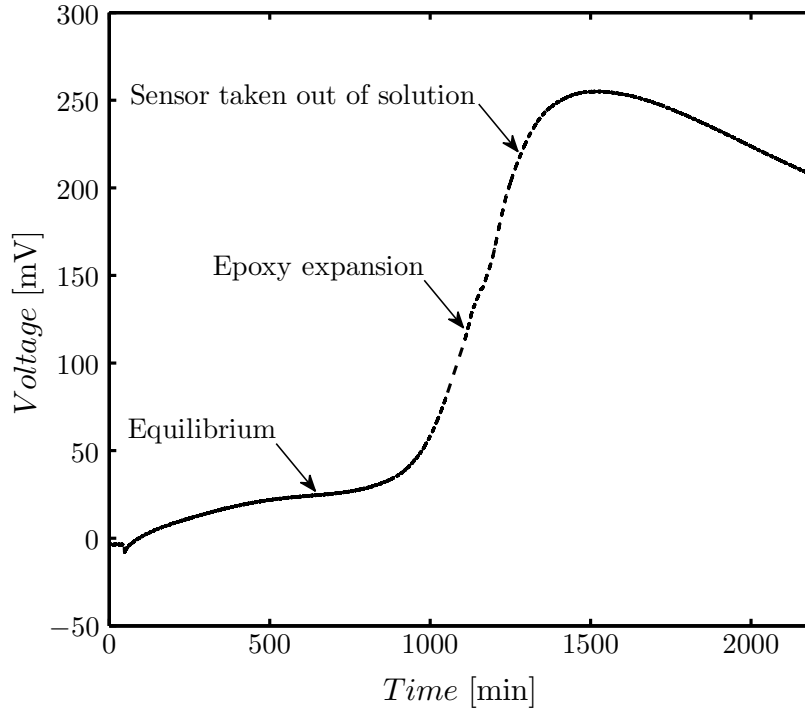


Figure 4-22: Sensor of procedure 2 in pH buffer 2.34

rect): For sample 1, thickness $\delta_1=61 \mu\text{m}$ and constant time $\tau_1 = 60$ minutes, the ratio $(\frac{\delta_1}{\delta})^2=(\frac{61}{200})^2=0.093$, and $\frac{\tau_1}{\tau}=\frac{60}{420}=0.143$. For the sample 2, thickness $\delta_1=77 \mu\text{m}$ and constant time $\tau_1 = 90$ minutes, the ratio $(\frac{\delta_2}{\delta})^2=(\frac{77}{200})^2=0.148$, and $\frac{\tau_2}{\tau}=\frac{60}{420}=\frac{90}{420}=0.214$. The results do not fit to equation (3.14). The determined thickness of the hydrogel sample may be wrong. According to these calculations, the hydrogel thickness should be around $160 \mu\text{m}$. This problem may come from the method to determine thickness of hydrogel in cavity. In this particular case, a microscope was used to manually evaluate the thickness inside the cavity due to unexpected broken profilometer as used for other measurement. Continuous rising in voltage of sensor of procedure 2 may happen due to the expansion of two components epoxy (same possible reasons to cause membrane to be broken in procedure 1. Epoxy may contain hydrophilic groups in its structure, resulting in an expansion when staying long time in solution. Other kind of waterproof glue without expansion should be applied in steps of packaging to glue components together.

Procedure 3: Results from procedure 3 are showed in figure 4-25 with two sensors

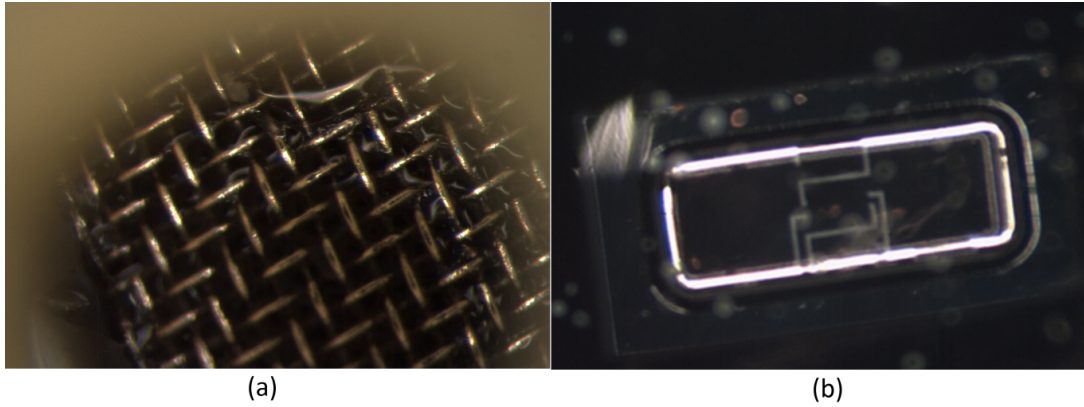


Figure 4-23: A photo from back side of the sensor through the hole on PCB and substrate: hydrogel inside the pressure sensor covered by stainless steel porous membrane (a), visible membrane of pressure sensor through silicone layer (b)

1 and 2. In this procedure, paraffin wax and silicone were used to join all the components of the sensor system together instead of two components epoxy as described in detail in figure 4-17. Results from sensor 1 shows that voltage signal increased at first but quickly went down and remain stable even the sensor was changed to higher pH buffer. This means silicone membrane of sensor did not receive expansion signal from the gel. The same problems happened to sensor 2 since the voltage signal did not change when sensor was dipped in the pH buffer 2.34 and even higher pH buffers. The reasons accounted for these phenomena may be the fact that paraffin wax together with silicone cannot hold the porous membrane close enough to the sensor. Therefore no pressure exerted toward the silicon membrane.

4.4 Conclusion

A hydrogel based pressure sensor was designed and constructed and the results from chapter 4 suggests a working principle in which a hydrogel can generate pressure causing the silicon membrane of the sensor to deform. The increased pressure due to swelling can be attributed the osmotic pressure, whereas negative pressures can be attributed physical forces pulling the membrane down below the displacement indicating the zero pressure equilibrium state. Due to the difficulties experienced from the suspected swelling of the packaging materials, an alternative method of

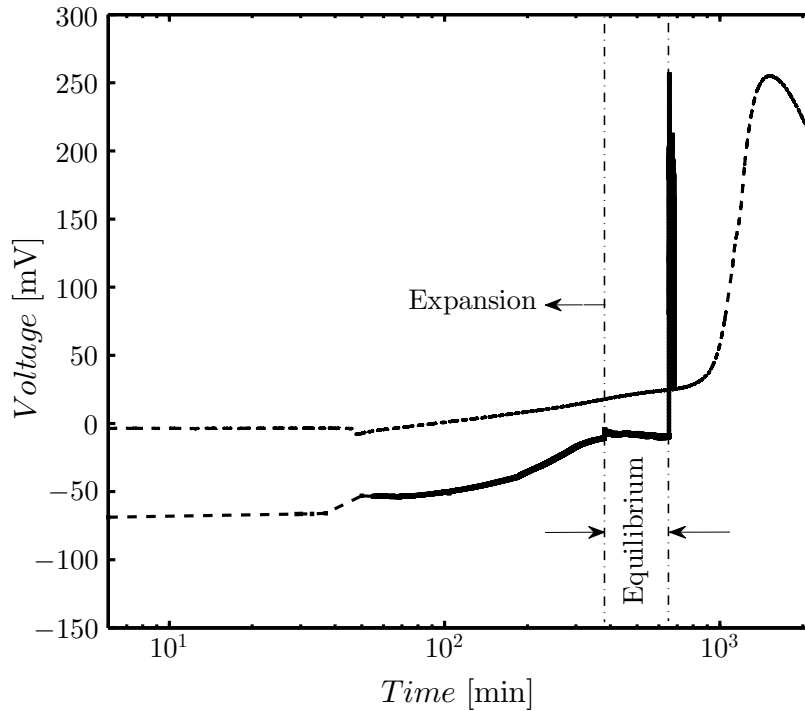


Figure 4-24: A comparison between signals of sensors in procedure 1 and 2

assembling the hydrogel sensor was described. A prerequisite for the sealing and encapsulation materials is that they should be waterproof and not to expand when staying a long time in solution. Regarding the response time of the gel, this can be reduced by implementing a custom made pressure sensor in which the thickness of the cavity that hydrogel layer is synthesized inside. The thinner hydrogel layer results in shorter diffusion distances. In the experiment, the specific hydrogel incorporated to the cavity of the pressure sensor reached the equilibrium after approximately 7 hours. Although the hydrogel gel sensor in this project did not work as expected according to the aim of making a pH sensor, it still demonstrated the ability of converting a signal of swelling or shrinking of a hydrogel to an electrical signal. In addition, several challenges in the packaging steps have been addressed for other future project to improve. We have reasons to believe that with several improvements in packaging sensor, pH -sensitive hydrogel sensor can work properly.

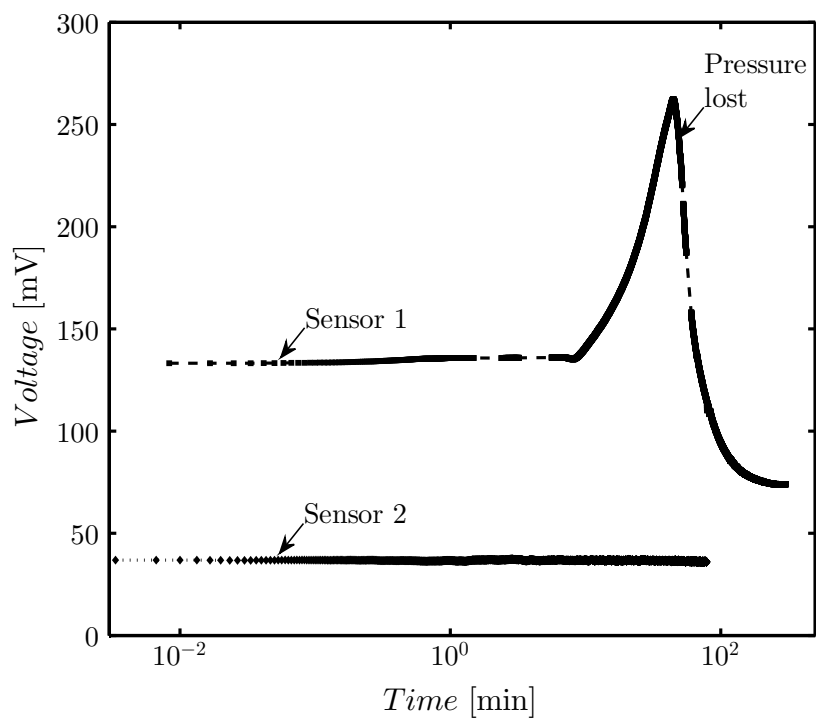


Figure 4-25: Sensors of procedure 3 in *pH* buffer 2.34, signal from sensor 1 and sensor 2

Chapter 5

Conclusion and Future work

5.1 Conclusion

This project focuses on developing a pH -sensitive hydrogel based micro-sensor, especially for human applications to measure the pH change inside living tissue. The optimal pH for tissue working properly is 7.4 and may be reduced to around 6.6 due to diseases. So the hydrogel sensor was supposed to work and detect the change of pH in the range of 6-8. The pH -sensitive hydrogel sensor is based on the corporation of HEMA-co-AA into the cavity of a piezoresistive pressure sensor. The hydrogel was chosen deliberately relied on its suitable properties and safety reasons. The hydrogel was individually investigated before incorporating into the pressure sensor. In order to study the behaviors of the hydrogel in micrometer scale, the hydrogel was synthesized inside a micro-fabricated cavity. Within a cavity, hydrogel can only perform its swelling and shrinking in one direction, allowing us to measure the changes in thickness of the hydrogel instead of the changes in volume of the hydrogel in different pH buffers. A profilometer was utilized to determine the changes in thickness of the hydrogel responding to pH solutions. The cavity was fabricated by photolithography techniques to form cavity with 1400 μm sides and 100-150 μm depth. There were two different processes to be attempted to fabricate this cavity. The first process to create SU8 wall on a silicon wafer (SU8-silicon) and the other is to form SU8 wall on a SU8 base (SU8-SU8). However, SU8-silicon could not support very well for those studies

on the hydrogel behaviors due to a difference in adhesion of the hydrogel sample to the SU8 wall and silicon bottom, resulting in buckling when the sample swelled drastically in pH buffers higher than 7. The results for characterization of the hydrogel HEMA-co-AA in this project were mostly based on using the SU8-SU8 cavity. The pH buffers PBS from 2-12 was prepared from phosphoric acid and its phosphate salts and was adjusted the ionic strength to 0.2 mM by sodium chloride.

The change of the hydrogel was observed under the microscope showed that when the hydrogel expanded in a constraint cavity, it tended to generate creases on the surface instead of a flat surface as in free expansion. For the hydrogel samples with thickness from 61,77 μm , the equilibrium status were reached mostly after 60, 90 minutes, respectively. These hydrogel samples demonstrated the expansions compared to the initial volumes at dry status of 55-77% at low pH 2-4 and expansions of 130-195% at higher pH 5-11. They got the equilibrium with pH above 7. The thickness of the sample influence not only the equilibrium time but also the maximum expansion of the hydrogel. There was a hysteresis on the hydrogel HEMA-co-AA behavior to be recorded in the experiments when increasing and decreasing pH of buffers at pH below 8. These phenomena can be accounted for a delay of the protonation to the deprotonation of functional acid groups inside the gel and other reasons from complicated kinetic of the hydrogel. The hysteresis of the hydrogel reduces when the recorded time is close to the equilibrium time. Thus, it can be avoided by measuring the signals at the equilibrium status. Short measuring-time (less than equilibrium time) for the swelling of the hydrogel can cause a light shift on curve of the behavior of the hydrogel to a higher range of pH . In addition, short measuring-time could not make the results for difference in expansion degree of different ratio in molar of HEMA-co-AA become clear in these experiments. Moreover, experimental works showed that hydrogel HEMA-co-AA after hydration should be stored in a suitable pH buffer 2-3.

The hydrogel after characterization was synthesized inside a cavity of the micro piezoresistive pressure sensor to make it become a pH -sensitive hydrogel based biosensor. The commercial SW415-2 pressure sensor was modified for a thinner cavity

before being incorporated with the hydrogel. A setup for electrical measurement was prepared, including PCB with dual op-amp, Labview software, etc. Electrical circuit, original SW415-2, and modified sensor were tested showing the perfect signals.

Hydrogel sensor underwent complex packaging procedures to connect it the external world and allow it to work in solution. The pressure sensor integrated with the hydrogel was placed and glued to a stainless steel porous membrane and together stuck to a chip carrier and then a PCB board. Gold wire bonds were bonded from the sensor to the chip carrier, chip carrier is linked with external wires by two component silver epoxy. Glob-top two components epoxy was applied to strengthen the wire bonds. Silicone was the waterproof outer layer to protect hydrogel sensor in solution. The initial packaging used two components epoxy Araldite 5min to join most of the components of the system. Hydrogel produced by this procedure worked in solution and proved that it is capable of converting the signal from expansion from the hydrogel in the solution to the electrical signal with the fact that the voltage increased corresponding to the expansion of hydrogel. It also showed that, for the specific synthesized gel in the experiment, the time for reaching equilibrium is around 7 hours. However, the hydrogel cannot stay long in solution for more than 20 hours due to the expansion of epoxy in solution, causing unexpected signal and even breaking the delicate membrane of pressure sensor. Another packaging procedure was built up to replace the previous packaging. Paraffin wax and silicone which known as waterproof material were used to join the components of the system instead of using two components epoxy Araldite 5min. The measurement system could not receive the signal of expansion of hydrogel from this sensor. A possible reason is that paraffin wax and silicone do not have strong adhesion to hold the porous membrane with the sensor.

Although the hydrogel sensor in this project did not work as expected to observe the pH changes in solutions, it showed the possibility to transduce physical changes of hydrogel to electrical signals. Future improvements in packaging steps will help to solve the problems remaining in this project.

5.2 Limitation

Some limitations of the project are mentioned here for further improvements in future. About the hydrogel HEMA-co-AA, even it performed a dramatic change in the pH range around 4-8 with determined pK_a approximately at 5.5-6. It is not an optimal choice because this pK_a is not so close to the pH of tissue living in normal condition (7.4) but HEMA-co-AA can be used as the model pH -sensitive hydrogel for developing a pH sensor.

5.3 Future work

The work has demonstrated a good performance of the hydrogel HEMA-co-AA and the ability of hydrogel sensor to transfer the swelling signal of the hydrogel to the electrical signal. There are some suggestions that can be made in the future. Firstly, it is necessary to fabricate a custom made piezoresistive pressure sensor. A fabricated sensor with thinner cavity can allow a synthesis of thinner hydrogel layer inside and thus a shorter response time of hydrogel. The thin hydrogel layer reaches the equilibrium status quicker and can help to reduce the hysteresis of the hydrogel behavior. Secondly, an improvement in the packaging of the hydrogel sensor should be figured out. The chemicals or adhesive components used in assembling of the hydrogel sensor should be waterproof and non-expansion in aqueous working environment. This is a decisive step to be able to record the signal from the sensor. Thirdly, since the experiments are conducted in room condition, effects of change of temperature and ambient pressure should be considered. We can make up a reference circuit to eliminate these changes of ambient temperature and pressure. Fourthly, other types of stimuli hydrogel can be interesting to study and incorporate to the piezoresistive pressure sensor such as ion-sensitive hydrogel, glucose-sensitive hydrogel, antigen-sensitive hydrogel, other kinds of pH -sensitive hydrogel, etc. HEMA-co-DMAEMA with pK_a around 7 which is closer to the pH of the living tissue should also be considered. Fifthly, model for simulation should be built up based on the theory of behavior of hydrogel to

predict the changes of the hydrogel both in free and constraint expansion-shrinkage. Sixthly, as the hydrogel is can be photo-sensitive, it can be photopatterned. A process to photopatterned should be attempted to produce the hydrogels in expected shape and thickness with the purpose for further integrating into different transducers.

Bibliography

- [1] J. W. Severinghaus, “Oxyhemoglobin dissociation curve correction for temperature and ph variation in human blood,” *Journal of Applied Physiology*, vol. 12, no. 3, pp. 485–486, 1958.
- [2] R. Miller and M. Pardo, *Basics of Anesthesia*. Elsevier Health Sciences, 2011.
- [3] L. Sherwood, *Human Physiology: From Cells to Systems*. Available Titles CengageNOW Series, Cengage Learning, 2008.
- [4] A. B. J. Groeneveld and J. J. Kolkman, “Splanchnic tonometry: a review of physiology, methodology, and clinical applications,” *J. Crit. Care*, vol. 9, no. 3, p. 198210, 1994.
- [5] G. A. B. Kolkman J. J., Otte J. A., “Gastrointestinal luminal pco2 tonometry: an update on physiology, methodology and clinical applications,” *British journal of anaesthesia*, vol. 84, no. 1, pp. 74–86, 2000.
- [6] S. Herber, *Development of a Hydrogel-based Carbon Dioxide Sensor: A Tool for Diagnosing Gastrointestinal Ischemia*. University of Twente [Host], 2005.
- [7] K. Gawel, D. Barriet, M. Sletmoen, and B. T. Stokke, “Responsive hydrogels for label-free signal transduction within biosensors,” *Sensors*, vol. 10, no. 5, p. 4381, 2010.
- [8] B. Zhao, , and J. S. Moore*, “Fast ph- and ionic strength-responsive hydrogels in microchannels,” *Langmuir*, vol. 17, no. 16, pp. 4758–4763, 2001.
- [9] A. GRAYSON, R. Shawgo, A. JOHNSON, N. FLYNN, Y. LI, M. J. Cima, and R. Langer, “A biomems review: Mems technology for physiologically integrated devices,” *Proceedings of the IEEE*, vol. 92, pp. 6–21, Jan 2004.
- [10] S. De, N. Aluru, B. Johnson, W. Crone, D. Beebe, and J. Moore, “Equilibrium swelling and kinetics of ph-responsive hydrogels: models, experiments, and simulations,” *Microelectromechanical Systems, Journal of*, vol. 11, pp. 544–555, Oct 2002.
- [11] R. Liu, Q. Yu, and D. Beebe, “Fabrication and characterization of hydrogel-based microvalves,” *Microelectromechanical Systems, Journal of*, vol. 11, pp. 45–53, Feb 2002.

- [12] D. T. Eddington, R. H. Liu, J. S. Moore, and D. J. Beebe, "An organic self-regulating microfluidic system," *Lab Chip*, vol. 1, pp. 96–99, 2001.
- [13] J. M. B. Q. Y. R. H. L. C. D. B.-H. J. David J. Beebe, Jeffrey S. Moore, "Functional hydrogel structures for autonomous flow control inside microfluidic channels," *Letters to Nature*, vol. 404, pp. 588–590, April 2000.
- [14] K.-F. A. Gerald Gerlach, *Hydrogel Sensors and Actuators: Engineering and Technology*. Springer, 2010.
- [15] Q. Thong Trinh, M. Guenther, J. Sorber, and G. Gerlach, "Hydrogel-based piezoresistive ph sensors: Modeling, simulation and experimental verification," in *Electronics Systemintegration Technology Conference, 2006. 1st*, vol. 2, pp. 1061–1070, Sept 2006.
- [16] G. Gerlach, M. Guenther, J. Sorber, G. Suchaneck, K.-F. Arndt, and A. Richter, "Chemical and ph sensors based on the swelling behavior of hydrogels," *Sensors and Actuators B: Chemical*, vol. 111112, pp. 555 – 561, 2005. Euroensors {XVIII} 2004The 18th European Conference on Solid-State Transducers.
- [17] S. Herber, J. Bomer, W. Olthuis, P. Bergveld, and A. Berg, "A miniaturized carbon dioxide gas sensor based on sensing of ph-sensitive hydrogel swelling with a pressure sensor," *Biomedical Microdevices*, vol. 7, no. 3, pp. 197–204, 2005.
- [18] Q. T. Trinh, G. Gerlach, J. Sorber, and K.-F. Arndt, "Hydrogel-based piezoresistive ph sensors: Design, simulation and output characteristics," *Sensors and Actuators B: Chemical*, vol. 117, no. 1, pp. 17 – 26, 2006.
- [19] L. Brannon-Peppas and N. A. Peppas, "Equilibrium swelling behavior of ph-sensitive hydrogels," *Chemical Engineering Science*, vol. 46, no. 3, pp. 715 – 722, 1991.
- [20] D. Chandrasekharaiah and L. Debnath, *Continuum Mechanics*. Academic Press, 1994.
- [21] S. K. De and N. Aluru, "A chemo-electro-mechanical mathematical model for simulation of ph sensitive hydrogels," *Mechanics of Materials*, vol. 36, no. 56, pp. 395 – 410, 2004. Coupled Chemo-Mechanical Phenomena.
- [22] H. Li, T. Y. Ng, a. Yong Kin Yew, and K. Y. Lam, "Modeling and simulation of the swelling behavior of ph-stimulus-responsive hydrogels," *Biomacromolecules*, vol. 6, no. 1, pp. 109–120, 2005. PMID: 15638511.
- [23] R. Berry, S. Rice, and J. Ross, *Physical chemistry*. Wiley, 1980.
- [24] J. Malmivuo and R. Plonsey, *Bioelectromagnetism: Principles and Applications of Bioelectric and Biomagnetic Fields*. Oxford University Press, 1995.

- [25] H. T. Tien and A. Ottova-Leitmannova, eds., vol. 5 of *Membrane Science and Technology*. Elsevier, 2000.
- [26] S. Payen, “Integration of hydrogels and plastics into microfabrication processes towards a mems rf-interrogated biosensor,” 2007.
- [27] M. S. T. Wallmersperger, “Modeling and simulation of the electro-chemical behavior of chemically stimulated polyelectrolyte hydrogel layer composites,” *Journal of Intelligent Material Systems and Structures*.
- [28] B. Kang, Y. dong Dai, X. hong Shen, and D. Chen, “Dynamical modeling and experimental evidence on the swelling/deswelling behaviors of ph sensitive hydrogels,” *Materials Letters*, vol. 62, no. 19, pp. 3444 – 3446, 2008.
- [29] D. C. M. Kamlesh J. Suthar and M. K. Ghantasala, “Swelling characteristics of 3d-arbitrary-geometry of the ph-sensitive hydrogels,” *ASME 2013 Conference on Smart Materials, Adaptive Structures and Intelligent Systems*, vol. 2, 2013.
- [30] D. C. M. Kamlesh J. Suthar and M. K. Ghantasala, “The swelling responsiveness of ph-sensitive hydrogels in 3d arbitrary shaped geometry,” *TECHNICAL PAPERS AND PRESENTATIONS*, 2013.
- [31] J. F. J. Dippy, S. R. C. Hughes, and A. Rozanski, “498. the dissociation constants of some symmetrically disubstituted succinic acids,” *J. Chem. Soc.*, pp. 2492–2498, 1959.
- [32] A. Richter, G. Paschew, S. Klatt, J. Lienig, K.-F. Arndt, and H.-J. P. Adler, “Review on hydrogel-based ph sensors and microsensors,” *Sensors*, vol. 8, no. 1, p. 561, 2008.
- [33] N. F. S. Jr., M. J. Lesho, P. McNally, and A. S. Francomacaro, “Microfabricated conductimetric ph sensor,” *Sensors and Actuators B: Chemical*, vol. 28, no. 2, pp. 95 – 102, 1995.
- [34] A. Richter, A. Bund, M. Keller, and K.-F. Arndt, “Characterization of a microgravimetric sensor based on ph sensitive hydrogels,” *Sensors and Actuators B: Chemical*, vol. 99, no. 23, pp. 579 – 585, 2004.
- [35] C. Ruan, K. Zeng, and C. A. Grimes, “A mass-sensitive ph sensor based on a stimuli-responsive polymer,” *Analytica Chimica Acta*, vol. 497, no. 12, pp. 123 – 131, 2003.
- [36] M. J. Lesho and N. F. S. Jr, “A method for studying swelling kinetics based on measurement of electrical conductivity,” *Polymer Gels and Networks*, vol. 5, no. 6, pp. 503 – 523, 1998.
- [37] S. Herber, W. Olthuis, P. Bergveld, and A. van den Berg, “Exploitation of a ph-sensitive hydrogel disk for {CO₂} detection,” *Sensors and Actuators B: Chemical*, vol. 103, no. 12, pp. 284 – 289, 2004. The 17th European Conference on

Solid-State Transducers, University of Minho, Guimares, Portugal, September 21-24, 2003.

- [38] S. Herber, J. Eijkel, W. Olthuis, P. Bergveld, and A. van den Berg, "Study of chemically induced pressure generation of hydrogels under isochoric conditions using a microfabricated device," *The Journal of Chemical Physics*, vol. 121, no. 6, 2004.
- [39] M. Guenther and G. Gerlach, "Hydrogels for chemical sensors," in *Hydrogel Sensors and Actuators* (G. Gerlach and K.-F. Arndt, eds.), vol. 6 of *Springer Series on Chemical Sensors and Biosensors*, pp. 165–195, Springer Berlin Heidelberg, 2010.
- [40] Sensoror-Norway, "Data sheet product brief of sw415-2 pressure sensor," *Datasheet*, 2004.
- [41] O. Krushinitskaya, *Osmotic sensor for blood glucose monitoring applications*. Doctoral thesis, 2005.